

PART IV

MOTION AND EXCITATION IN THE  
CHROMOSPHERE

# MOTIONS OF CHROMOSPHERIC FINE STRUCTURES

EDWARD N. FRAZIER

*Aerospace Corporation, Los Angeles, Calif. 90009, U.S.A.*

**Abstract.** This review concerns itself with the measurement of the effects of chromospheric motions and the diagnosis of those motions themselves over approximately the last ten years. The different types of observational techniques are described. The different size regimes of motions are reviewed and their possible effects on observable quantities are discussed. The different types of motion in the lower chromosphere are reviewed, including microturbulence, 'layered' motions, and observations and interpretation of asymmetries in the core of the Ca II K line. The observation of motions in H $\alpha$  mottles on the disk and spicules on the limb are reviewed, from the standpoint of both line profile analysis and broad-band measurements. The interpretation of these motions and attempts to construct empirical models of chromospheric fine structures are discussed.

## 1. Introduction

A review of motions of chromospheric fine structures is a little difficult because motion is such a fundamental property of the fine structures. In fact, the most important single aspect of these fine structures is that they are dynamic, not static phenomena. Thus, motions should really be discussed only as an integral part of the general problem of fine structures, and indeed, we have seen discussions of motions being raised throughout this symposium in relation to every other aspect of the overall fine structure problem, as they should have been. However, for purely organizational reasons, this review will be limited to the observations of motions *per se*; how they are observed, what the results are, where the discrepancies and unresolved questions lie, and what should be done to further clarify the state of motion of the chromosphere.

I shall start with a brief summary of general observational techniques and a crude attempt to provide an organizational framework for considering the various phenomena according to their sizes. Consideration of the specific problems themselves are grouped according to that most unnatural separation; disk and limb. Finally I attempt to rectify that sin and provide as unified as possible a picture of chromospheric motions.

## 2. Techniques

### 2.1. OBSERVATIONAL TECHNIQUES

One should start by realizing that there are four main independent variables, or coordinates, each of which are important in the measurement of motions;  $\lambda$ ,  $x$ ,  $y$  and  $t$ . Historically, observations have fallen into three broad categories which can be distinguished by the coordinates that are well resolved. These can be seen in Table I. It is important to note that historically the analysis of the data in each category has been specialized and developed almost independently of the other categories. Only recently have there been observational and analytical techniques developed which tend to eliminate the artificial boundaries between these categories.

TABLE I  
Categories of instrumental techniques

Category	Resolved coordinate	Instrumental example
'Profile-blind' mapping	$x, y, t$	Filtergrams, spectroheliograms
Low resolution line profiles	$\lambda$	Photoelectric spectra
High resolution line profiles	$\lambda, x$	Photographic spectrograms
Improvements or combinations	$\left\{ \begin{array}{l} x, y, t, (\lambda) \\ \lambda, x, t \\ \lambda, x, y, (t) \\ \lambda, x, y, t \end{array} \right.$	Tunable filters
		Time-sequence spectrograms
		'Stepped' spectrograms
		Image slicer w/spectrograms, Multi slit spectrograph

The first category is what might be called 'profile blind' mapping. Filtergrams and spectroheliograms are the prime examples. Such observations are poorly suited for the deduction of local physical variables, because they contain no information about the line profile, but they are an excellent means of *discovering* dynamical phenomena and identifying their general nature. For example, such phenomena as the 5-min oscillations, the supergranulation and Moreton waves were discovered with this technique (Leighton *et al.*, 1962; Athay and Moreton, 1961), so we may expect profile blind mapping to remain at the forefront (and *only* at the forefront) of further study of dynamic phenomena.

Low (spatial) resolution profiles have been virtually forced upon us by those who recognized the need for first achieving a first order theory of the structure and radiation of the chromosphere. Since there is no real instrumental requirement that maintains this separate category, one should expect that when the first order chromosphere is understood this category will be allowed to pass into history. Indeed, since most of the recent articles on chromospheric radiation have dealt with inhomogeneities in one way or another, we might be able to say that this time has already arrived.

The category of high (spatial) resolution profiles has had a long history observationally but the analysis of the data has lagged behind, awaiting the completion of category two. An important observational improvement to this category is the use of reflecting entrance slits viewed through narrow band filters. This enables one to at least identify which type of spectral feature is under study.

There are a number of technical improvements which lead to combinations or extensions of these categories. They are listed in Table I without detailed comment. There are two general comments that should be made however. First, one can see that it is technically quite possible to obtain data that is a function of all the principal independent variables. This should free us from the need to tailor the analysis technique to the instrumental limitations. Secondly, this 'fully generalized analysis' has not yet really come to fruition. Why not? Simply stated, because no one seems to know what to do with all that data. The volume of data is massive and the data reduction

problem is serious. This can be solved however with enough money and effort. What is really needed is a sound theoretical framework within which one can analyze all these fluctuations.

## 2.2. SIZE SCALES AND REGIMES

Continuing in the same spirit as in the previous section, I would now like to categorize the various possible motions according to their sizes, since their size largely determines the visible effect that they will produce. We probably are all familiar with the three classical size regimes; microturbulence, unresolved macroturbulence and macroturbulence. The dividing boundary between these regimes is the mean free path of a line photon,  $L$ , and the instrumental resolution element,  $R$ , respectively. (cf. de Jager, 1959, p. 93). Since the term macroturbulence connotes an additional property to mass motions which no longer seems appropriate, it would seem preferable to change the names of the last two categories to simply 'unresolved mass motion' and 'mass motion', respectively. Note that the boundary between these last two categories refers only to a horizontal plane. In the vertical plane we have a different situation (referring only to disk observations now). The intermediate regime becomes what might best be called 'layered motion', and the boundary between this regime and that of mass motion becomes an ill-defined quantity which is probably best called, 'the thickness of a line forming layer',  $\Delta z$ . So there are four regimes, depending on the horizontal and vertical size scale of the motion, and two of these regimes (layered motion and unresolved mass motion) overlap each other considerably. Only in the simplest regime – mass motion – is one justified in making a one-to-one correspondence between Doppler shift and line-of-sight motion. To infer velocities in the other regimes, one must postulate a complete model of the moving elements, calculate the emergent radiation (taking into account the radiative interaction between the elements) and adjust the model parameters to fit the observed profiles. Since this is a tedious procedure, and does not guarantee uniqueness, it is usually ignored.

One can make rough estimates of which regimes contain chromospheric motions. For strong chromospheric lines,  $L \approx 10^2$  km, for most spectrographs, the best  $R$  is about  $10^3$  km.  $\Delta z$  is ill-defined, but from the results of Kulander and Jefferies (1966) and Athay (1970) we take  $\Delta z \approx 5 \times 10^2$  km. These numbers should not be taken too seriously for several reasons. The boundaries are not all sharp; not only are they very broad, there is presently no theory to tell us how broad they are. Furthermore, these boundaries vary considerably as a function of the instrument used, the seeing, the line used and even the feature viewed. Despite these uncertainties, it is readily apparent that *all* four regimes will contain significant chromospheric motions.

First, let us consider microturbulence, and what its status is in the chromosphere. First, should we expect it to exist? Yes. Theories of acoustical generation in the convection zone predict the possibility of sound waves with wavelengths as short as a kilometer. Crude estimates based on viscous dissipation of turbulent eddies predict eddy wavelengths as short as a meter! We don't know for sure if it is there, but we really should expect it. Secondly, can we observe it in the chromosphere? Not in the

classical sense. By original definition it is observable only by its effect on equivalent widths, but the curve of growth method and its descendant, the Goldberg-Unno method are inappropriate for chromospheric studies. However, the concept is preserved by the study of synthetic line profiles through the use of the usual equation in computing Doppler broadening:

$$\Delta\lambda_D = \frac{\lambda_0}{c} \left[ \frac{2kT}{m} + \xi_t^2 \right]^{1/2} \quad (1)$$

$\xi_t$  is the microturbulent velocity and is the parameter specifying one component of a Maxwellian velocity distribution:  $f(\xi) = (1/\pi^{1/2}\xi_t) \exp(-\xi^2/\xi_t^2) d\xi$ . Thus, microturbulence is treated by assuming that there is no formal difference between turbulent motions and thermal motions, a situation which has not changed in nearly forty years.

The intermediate regimes, particularly unresolved mass motion, have frequently been lumped in with microturbulence under the heading of 'non-thermal motions'. This really should not be done because the use of Equation (1) assumes a gaussian distribution, which is clearly invalid for the larger scale motion. Work has proceeded on these regimes recently however, through the study of multi-component models. Here, specific models of differentially moving elements have been postulated (or inferred from observations of the size and amplitude of inhomogeneities) and the radiative transfer through such models has been solved explicitly. This technique has been applied to the analysis of both unresolved mass motions, through the use of two and three-column models, and to layered motions through the use of models with differentially moving layers. The results are still very numerical and too specific to constitute a general analysis technique of these intermediate regimes, but the progress is encouraging. The specific models will be discussed in the following sections.

A word about asymmetries, which seem to be fairly ubiquitous companions to velocity studies. Velocities alone do not produce asymmetries. Asymmetries are produced when other local physical variables fluctuate in correlation with velocities. Since these variables obviously are a function of height, layered motions almost invariably produce asymmetries. Almost by definition, resolved mass motions should not produce asymmetries. The other two regimes, however, are not so clear. Asymmetries may or may not be present depending on the details of the temperature-pressure-velocity relationships. This calls for a much broader attack on the problem than the mere consideration of the size and amplitude of the motions.

### 3. Disk Phenomena

#### 3.1. MICROTURBULENCE

We start the study of disk phenomena with a brief review of the first order chromosphere, and this means microturbulence. The most logical place to start is with low resolution profiles. This approach measures the total power contained in *all* the regimes and calls it microturbulence or 'non-thermal motions'.

### 3.1.1. Low Resolution Studies

The most appropriate starting point is probably the review by de Jager (1959) in which all the then available values of  $\xi_t$  are collected. There it was shown that all measurements were in reasonable agreement with a linear rise of  $\xi_t$  from about  $3 \text{ km s}^{-1}$  at  $h=0$  to about  $15 \text{ km s}^{-1}$  at  $h=3000 \text{ km}$ . This result includes a number of different observations, techniques, and resolutions. Can we believe it? I think that if you keep in mind that microturbulence is essentially a category for 'leftovers' you can see that this result is useful as an upper limit. Our job now is to see how far down we can pull this curve.

There is a fairly reliable measurement in the region of the temperature minimum. Canfield (1969, 1971) measured the half-widths of rare Earth lines formed in the wings of the H and K lines. This is a rather pretty measurement because (1) he showed that they are formed at the same height as the H and K wings, (2) the lines are weak, so the measured Doppler widths are the actual Doppler widths, (3) being so massive, these ions have a thermal speed much less than the turbulent speed. His results can be seen in Figure 1 (Canfield, 1971):  $\xi_t$  is about  $2 \text{ km s}^{-1}$  throughout the temperature minimum. This is still an upper limit, since this refers to power from all the regimes.

Higher in the chromosphere there is a result from analyses of the O I  $\lambda 1304.9 \text{ \AA}$  line. Athay and Canfield (1969), using a model with a microturbulence of  $6\text{--}7 \text{ km s}^{-1}$ , had predicted that this line should show a strong central reversal. However the observations show it to be nearly flat-topped. Jones and Rense (1970) concluded that, in addition to the microturbulence, a macroturbulence (unresolved mass motion) was necessary for the model to reproduce the flat top. The best fit was achieved with unresolved mass motion of  $6.8 \text{ km s}^{-1}$  (Figure 2).

Throughout the chromosphere one can infer  $\xi_t$  from synthetic models whose parameters are adjusted to fit various sets of observational data. Fitting the profiles of the Ca II H and K lines is the classic problem, and the homogeneous case seems to have reached the ultimate in the review paper by Linsky and Avrett (1970). To reproduce the wide Ca II profiles a turbulent velocity is incorporated into the model as shown in Figure 3. A much more ambitious model (Vernazza *et al.*, 1973) seeks to fit a number of hydrogen, carbon and silicon lines as well as EUV and microwave continuum data. In this model a similar turbulent velocity is derived (the Vernazza *et al.* turbulence is slightly higher in the upper chromosphere).

It should be noted that, for consistency, both these models incorporate a 'turbulent pressure' term:

$$P_{\text{total}} = P_{\text{gas}} + P_{\text{turb}}, \quad P_{\text{turb}} = \frac{1}{2} \rho \xi_t^2. \quad (2)$$

In the mid-chromosphere  $P_{\text{turb}}$  is an order of magnitude smaller than  $P_{\text{gas}}$  or less, and so has a negligible effect on the model. But at heights of about  $2000 \text{ km}$ ,  $P_{\text{turb}}$  becomes almost as great as  $P_{\text{gas}}$  and thus increases the scale height in this region. The result of this is to raise the altitude of the transition zone. The magnitude of this altitude shift is  $300 \text{ km}$  in the Vernazza *et al.* model. So it appears that the inferred existence of high

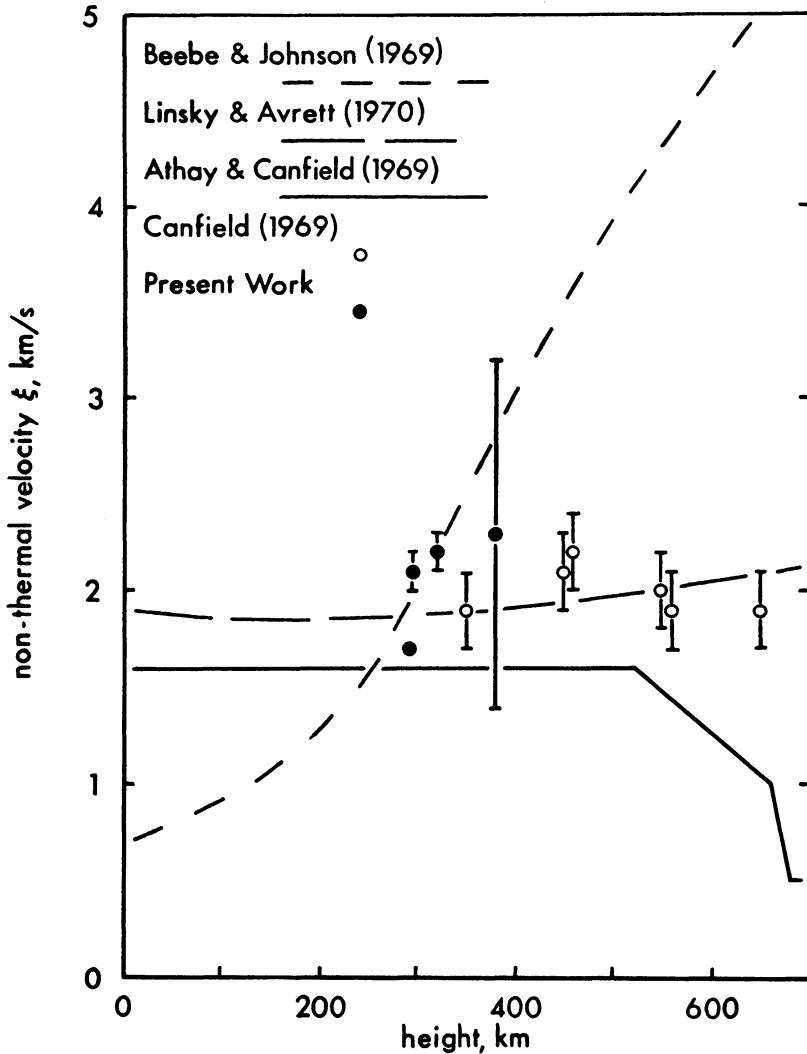


Fig. 1. The 'non-thermal velocity' as determined from the half-widths of rare Earth lines in the low chromosphere (from Canfield, 1971). The dashed lines refer to models used in synthetic K line profile calculations.

turbulent velocities (greater than about  $\xi, \approx 7 \text{ km s}^{-1}$ ) in the upper chromosphere can be tested by observations of the altitude of the transition region, if sufficient height resolution can be achieved.

### 3.1.2. Inhomogeneous Models

There have been a number of two or three component models of the chromosphere, all of which employ microturbulence as a free parameter. All of these models suffer from a profusion of adjustable parameters, and therefore cannot be claimed to be

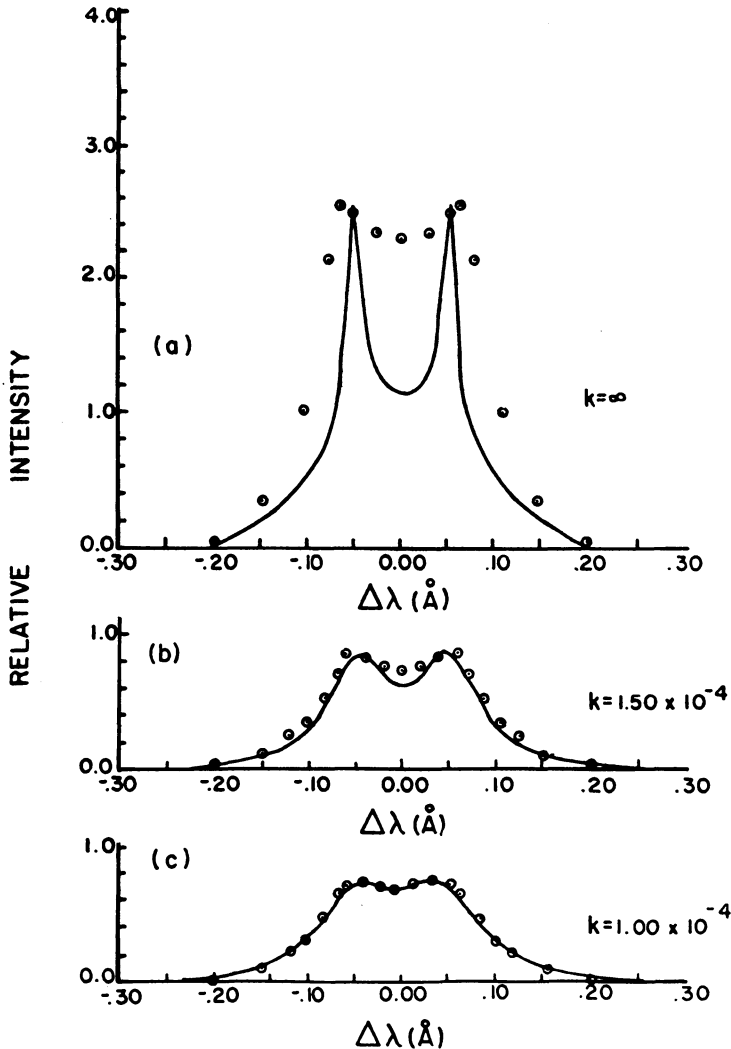


Fig. 2. The effect of unresolved vertical mass motions on the profile of the O I  $\lambda 11304.9$  Å line (from Jones and Rense, 1970). The circles represent the observed relative solar profile; the solid lines are the calculated profiles.

$$k = \frac{1}{2\xi^2}. \text{ For } k = 10^{-4}, \xi \approx 7 \text{ km s}^{-1}.$$

unique. Beebe and Johnson (1969) and Beebe (1971) build a purely geometrical two component model for the emission of the K line and, after settling on a  $T_{\min}$  of 4200 to 4300 K, infer reasonably small (depth and space dependent) values of  $\xi$ , (Figure 4). Wilson (1970) builds a three component model with very large values of  $\xi$ . The need to consider explicitly the radiative interaction between the various components of such models has led to a series of papers in which a method of solving the two-dimensional equation of radiative transfer has been developed (Cannon, 1970, 1971a, 1971b; Cannon and Rees, 1971). This method was applied to the interpretation of

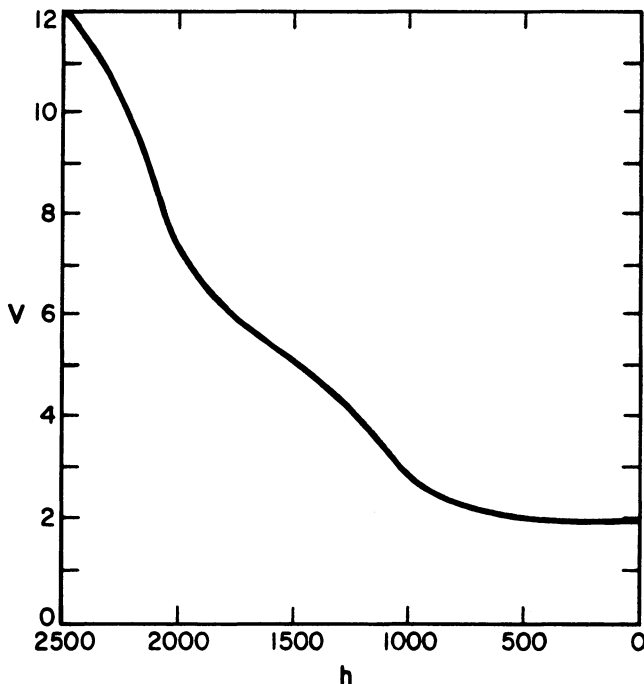


Fig. 3. The microturbulence used in a homogeneous model to synthesize the profiles of the calcium lines (from Linsky and Avrett, 1970).

observed fluctuations in the low chromosphere in terms of local density temperature and velocity fluctuations.

Cram (1972) has computed a self-consistent two component model for the K line *in the cell interiors only*. The two components correspond to (1) a background or cell component with a monotonically decreasing source function and (2) a  $K_2$  bright-point

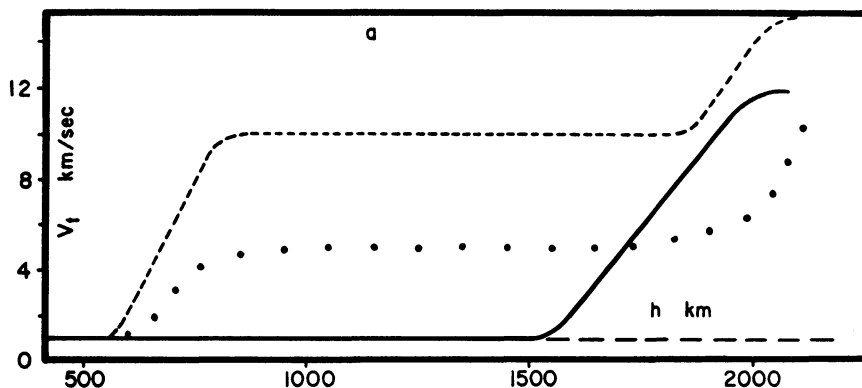


Fig. 4. The turbulent velocities used in a two-component model of the K-line profile (from Beebe, 1971). The dotted line represents the turbulence in the wall or network component, the solid line is the turbulence in the cell component. The dashed lines represent two other test models.

component. With the explicit inclusion of layered motions, reasonable agreement with observations is achieved with  $\xi_t = 5 \text{ km s}^{-1}$  in the 'bright' component and  $\xi_t = 7 \text{ km s}^{-1}$  in the 'cell' component.

All these models have the common advantage of easily reproducing the limbward behavior of the K line (both darkening and broadening) in spatially averaged profiles. However at disk center, the individual components of these models should be compared directly with high resolution spectra. It makes a little sense to average several synthetic profiles, average spectra over a large area, then compare the two.

### 3.1.3. Summary

In summarizing the actual results on microturbulence the major difficulty lies in separating it from the other regimes, principally unresolved mass motion on the one side, and simple temperature effects on the other side. In separating microturbulence from unresolved mass motions, I have been able to find only one possibility; the analysis of central reversals (or absence thereof) in the chromospheric lines other than H and K. The example of the O I  $\lambda$  1304.9 line quoted above is the prototype. It appears that the further addition of microturbulence cannot remove a predicted central reversal and that unresolved mass motion is necessary to reproduce the flat topped profile. Separation of  $\xi_t$  and  $T_e$  still appears to be done best by fitting a model to as wide as possible a set of observational constraints (e.g. H and K profiles, EUV and microwave emission). This is a rather arbitrary process though, and it is an open question whether or not it can survive the inclusion of inhomogeneities into the problem.

There are conflicting indications of spatial variations of  $\xi_t$ . Beebe (1971) finds a higher  $\xi_t$  in the network while Wilson (1970) requires a lower  $\xi_t$  there. Mein (1971), in his analysis of the infrared Ca II lines finds no change in  $\xi_t$  from cell to network. This question will certainly become a very important one as the fundamental difference between cell and network regions becomes more widely appreciated.

It is tempting to collect all the inferred values of  $\xi_t$  on one figure and draw a smooth curve through all the points, but that is premature now. Instead, Figure 5 just illustrates schematically the broad path where the various values are generally found. The sound speed is included for comparison. About all that can be said about the numerical value of microturbulence at this time is that it is very roughly Mach 0.2 to 0.3 throughout the chromosphere. Aside from the well-known defects in the theoretical foundation of microturbulence, there seem to be two main reasons for our present lack of accurate knowledge of microturbulence: (1) The spatial resolution of the various techniques varies greatly (e.g. what appears as microturbulence in one measurement is actually resolved mass motion in another measurement). (2) The inaccuracy introduced with the assumption of a homogeneous chromosphere is poorly known, and the possibility of spatial variations of  $\xi_t$  is not yet settled.

The idea of anisotropic turbulence has been around for a long time because nearly all Fraunhofer lines broaden toward the limb. The interpretation of this broadening is entangled to a certain extent with the height variation of  $\xi_t$ , but primarily with the

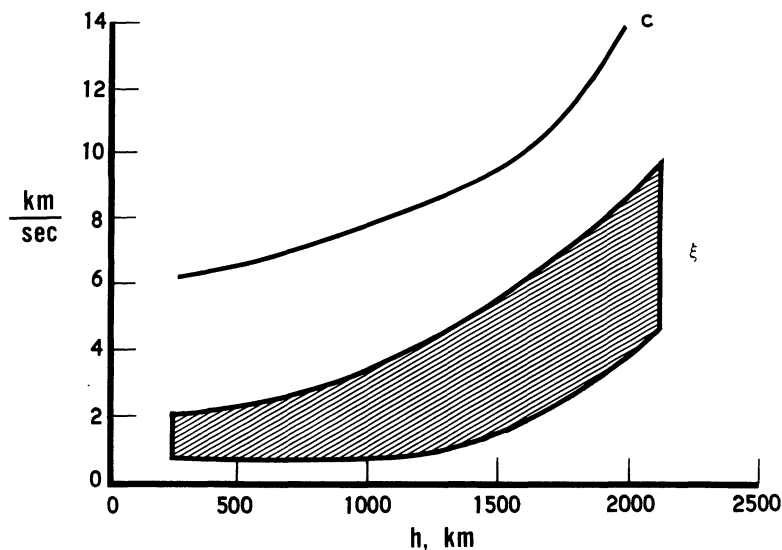


Fig. 5. Schematic summary of the various calculations of  $\xi_i$  in the chromosphere. All reasonable values fall roughly within the band denoted.  $c$  is the local sound speed.

effect of inhomogeneities. Both for the H and K lines and for the Na D lines (Wilson, 1973), it has been shown that the inclusion of inhomogeneities can completely reproduce the limb broadening. For this reason one can probably dismiss anisotropic turbulence.

### 3.2. LAYERED MODELS

There have been a number of studies concerning the effects of differentially moving layers. These have been motivated by an attempt to explain the asymmetries observed in H and K,  $H\alpha$  and other strong lines. These models are still very exploratory and numerical, but encouraging progress has already been made. We mention the work of Kulander and Jefferies (1966), Kulander (1976, 1968), Beckers (1968), Athay (1970a, b), Cannon and Rees (1971) and Cram (1972).

Differentially moving layers have two general effects on the line profile. First, the source function itself may be changed, and secondly, the emergent intensity is changed due to the shift of the absorption profile. Several of these studies have determined that if the layered motions have a magnitude less than the Doppler width of the line, and if the gradients in the velocity and the source function are small, then the source function is not significantly affected by the motion. In this case the source function from static models can be used; otherwise it must be computed explicitly. Of course the shift of the absorption profile always has a strong effect on the emergent intensity.

From the different numerical cases that have been studied, several general conclusions can be reached. First, only motions in the uppermost layers produce line shifts which could be accurately interpreted by means of, say, the line bisector technique. And this will be the case only if the moving layer is thick enough. For example, if a

layer comprising the entire region where the  $H\alpha$  core is formed is moving, then the entire  $H\alpha$  core will show an accurate Doppler shift; however as this layer becomes thinner, the inferred Doppler shift falls below the true one. In addition to this result, there is the more general result that height discrimination (by observing different parts of the line profile) is lost. More explicitly, "Motion far above  $\tau_v = 1$  may produce an apparent evidence of motion near  $\tau_v = 1$  and motion near  $\tau_v = 1$  may shift the profile at  $v$  by an amount corresponding to a velocity that is only a fraction of the true velocity." (Athay, 1970b).

If the moving layer occurs deeper, then the inferred velocity could be either smaller than or larger than the true velocity depending on whether the layer is located at  $\tau_v = 1$  or not, or whether the velocity gradient is positive or negative. Furthermore, if the source function and optical depth vary independently of the velocity, then the direct inference of velocities becomes so ambiguous that even velocities of the wrong sign can be inferred. In this case, it seems essential to postulate a model in which all of these quantities are free parameters, and then fit this model to the entire line profile.

Two authors, Athay and Cram, have had the courage to publish actual asymmetric K profiles which could be compared with real data. Although Cram's model is much more sophisticated than Athay's, they do agree that a  $K_{2v}$  feature can be reproduced by a rising intermediate layer or a falling top layer, probably the latter. In either case, the velocities needed are of the order of the sonic velocity. It also appears that velocity effects alone are insufficient to reproduce the observed profile accurately.

### 3.3. K LINE ASYMMETRIES AND FEATURES

The observational study of K line asymmetries has seen a considerable renaissance recently. The number of interesting new results, coupled with the theoretical studies of layered motion, make this one of the more fascinating fields of solar dynamics that exist today. We start with a summary of the observed statistics of asymmetries.

#### 3.3.1. *Asymmetry Statistics*

Three papers have investigated this topic recently (Bappu and Sivaraman, 1971; Liu and Smith, 1972; Pasachoff, 1970). We summarize their findings on Table II, which tabulates the percentage abundance of 5 rough classes of asymmetry. A separate sixth class includes the total absence of  $K_2$ . Since this sixth class is not mutually exclusive of the classes, 'no  $K_{2r}$ ' or 'no  $K_{2v}$ ', and since the authors use different terminology to report their results, there remains some ambiguity. However, some general trends can be noted. Viewing only the first two rows of Table II for the moment, we see that about one-half to three-quarters of all K profiles have double peaked profiles of some sort and that these profiles are found both in the network regions and in the cells. (The distribution between network and cell of these double peaked profiles may be very uneven however. This point has not yet been studied.) Of these profiles, the vast majority are asymmetric with the violet peak asymmetries outnumbering the red peak asymmetries roughly two to one. The remaining one-quarter to one-half of the profiles are missing one or both peaks *and are found preferentially within the cells*. Any

TABLE II  
The percentage abundance of the 5 qualitative classes of  $K_2$  asymmetries

	no $K_{2R}$	$I_{K_{2V}} > I_{K_{2R}}$	$I_{K_{2V}} = I_{K_{2R}}$	$I_{K_{2V}} < I_{K_{2R}}$	no $K_{2V}$	no $K_2$ AT ALL	SAMPLE SIZE
BAPPU AND SIVARAMAN (1971)	22.3 (dark $K_3$ cell)	45.3	4.7	25	0.7	0.7	1 FRAME 148 PROFILES
LIU AND SMITH (1972) (preferred location)	20 (cell)	50 (network, cell)			10 (cell)	20 DARK SPOT IN CELL	200 FRAMES
PASACHOFF (1970)	80	10			20	?	1 FRAME

dynamical model of the chromosphere should be capable of reproducing these facts.

The cause of the asymmetries seems to be indicated from further results of Bappu and Sivaraman. They found a significant correlation of these classes with the observed Doppler shift of  $K_3$  (Figure 6). This relation can be summarized with the interpretation that the asymmetry in  $K_2$  is caused by a Doppler shifted  $K_3$  component partially veiling one of the  $K_2$  components. The same effect was noted by Pasachoff although he did not establish an absolute wavelength scale. This is precisely the behaviour predicted by Athay (1970a). Although both Athay and Cram (1972) have shown that a  $K_2$  asymmetry can be produced either by a rising  $K_2$  layer or a falling  $K_3$  layer, the fact that  $K_3$  is Doppler shifted away from the bright  $K_2$  component indicates that the asymmetries are caused by motion in the  $K_3$  layer. That motion is then of rather large amplitude (10 to 20 km s<sup>-1</sup>) and predominantly downward.

There seems to be yet another feature in the K emission; the 'dark  $K_3$  regions'. Both Bappu and Sivaraman and Liu and Smith find that the class of 'no  $K_{2r}$ ' is correlated with a  $K_3$  component that is not only red shifted, but also unusually dark. In fact Liu and Smith find that in this feature  $K_{2v}$  is also absent, in contradiction to Bappu and Sivaraman. This point should be cleared up (although one should give greater weight to the results of Liu and Smith due to their much larger sample) before one tries to understand the physical nature of this type of region. If there is no  $K_2$  at all, then this could be the background component postulated by Wilson (1970) and Cram (1972), in which the source function actually decreases monotonically with height.

### 3.3.2. The Pasachoff-Zirin Model

The main discrepancy in the asymmetry statistics is that Pasachoff observed almost no double peaked profiles at all, and on the basis of this developed a radically different

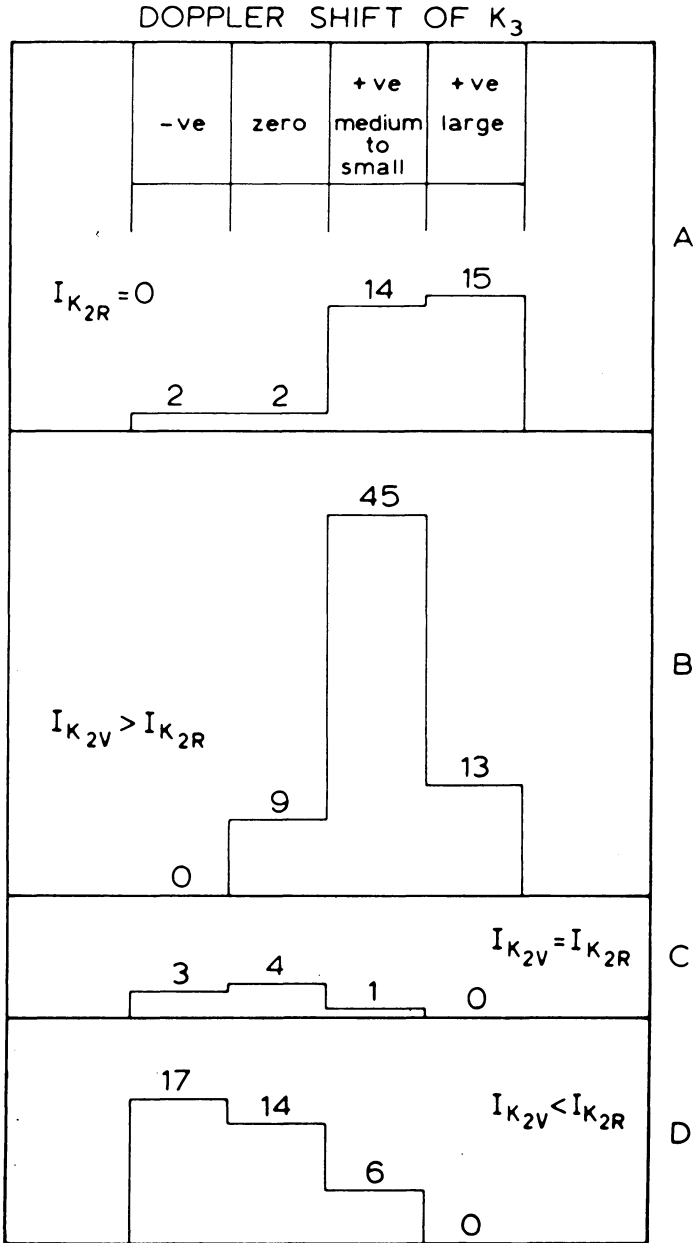


Fig. 6. Histograms of the Doppler shift of  $K_3$  grouped according to four of the  $K_2$ -asymmetry classes (from Bappu and Sivaraman, 1971). The numbers over the histograms represent the number of instances in each category. There is a definite correlation of the  $K_3$  Doppler shift with the sense of the asymmetry.

model of calcium emission originally proposed by Zirin (1966). This model consists of a basic profile which has little or no  $K_2$  emission, overlaid by small features which emit a single  $K_2$  peak. These features must possess a binary velocity distribution of  $\pm 10$  to  $20 \text{ km s}^{-1}$ . This model has been investigated by many people; the most recent and detailed study is that of Cram (1972). He shows that the model cannot reproduce the observed limbward separation of the peaks. The data is also contradicted by the other two observations and by Wilson and Evans (1971). Thus it seems fairly clear that, while occasional features may radiate by this model, it is inadequate as a general explanation for calcium emission.

The question arises as to how Pasachoff obtained such an atypical distribution of asymmetries. Skumanich *et al.* (1972), by comparing the distribution of broad-band brightnesses of Pasachoff's sample, showed that it was very deficient in bright network elements (i.e. the slit fell by chance almost exclusively across cell regions). Liu and Smith showed that the single peaked profiles strongly prefer cell regions, so this case is an excellent example of strong accidental bias of a small sample.

### 3.3.3. Time Behavior

While the theoreticians have just started to grapple with steady-state asymmetries, the observers have opened up a fascinating and fertile new chapter in the seemingly endless saga of the K line. The first indications that the asymmetries have complicated histories came from Wilson and Evans (1971) and Wilson *et al.* (1972), who reported instances of single peaks evolving into double peaks and vice versa. The time scales were as short as 15 s. Also, Liu *et al.* (1972) outlined the time history of  $K_{2v}$  bright points from a time sequence of  $K_{2v}$  spectroheliograms (Figure 7). The  $K_{2v}$  points rise in brightness in 20 to 30 s and seem to fade out even faster! The study of such features with time sequence spectrograms should be very fruitful. In fact Liu (1973) has just observed a very systematic time development of the K profile through these events. Samples of his spectra are shown in Figure 8. The subtracted profiles (profile at time  $t$  minus profile at time zero) of event *B* are shown in Figure 9. The brightening starts in the  $K_1$  wing, progresses in toward the center, produces a  $K_{2v}$  point, then fades out. The whole process repeats roughly every 180 s. Since  $K_3$  was not observed to brighten significantly, Liu interprets this type of event as a direct observation of deposition of wave energy at the level of  $K_2$  formation, i.e. the mid chromosphere. Further, since the 180-s period makes it fairly clear that this dissipation is the fate of the high frequency tail of the resonant oscillations, we can expect this behavior to be very common and to contribute significantly to the energy budget of the chromosphere.

### 3.4. $H\alpha$ MOTTLES

The discussion up to now has concerned itself with altitudes less than about 2000 km. It seems that around this height even a quasi-homogeneous chromosphere vanishes and one is left with only isolated features which are imbedded in the corona. This model has of course been developed from a much broader context, but it is equally valid and useful when considering  $H\alpha$  mottles.

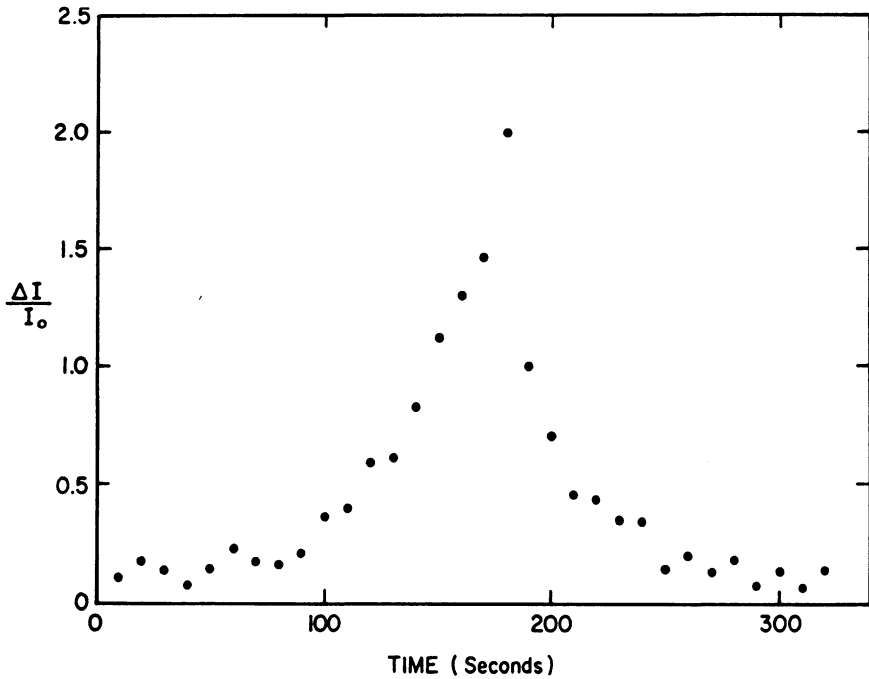


Fig. 7. The time history of the contrast  $\Delta I/I_0$  of a typical cell point on a  $K_{2v}$  spectroheliogram (from Liu *et al.*, 1972).  $I_0$  is the average intensity of the 'quiet' background.

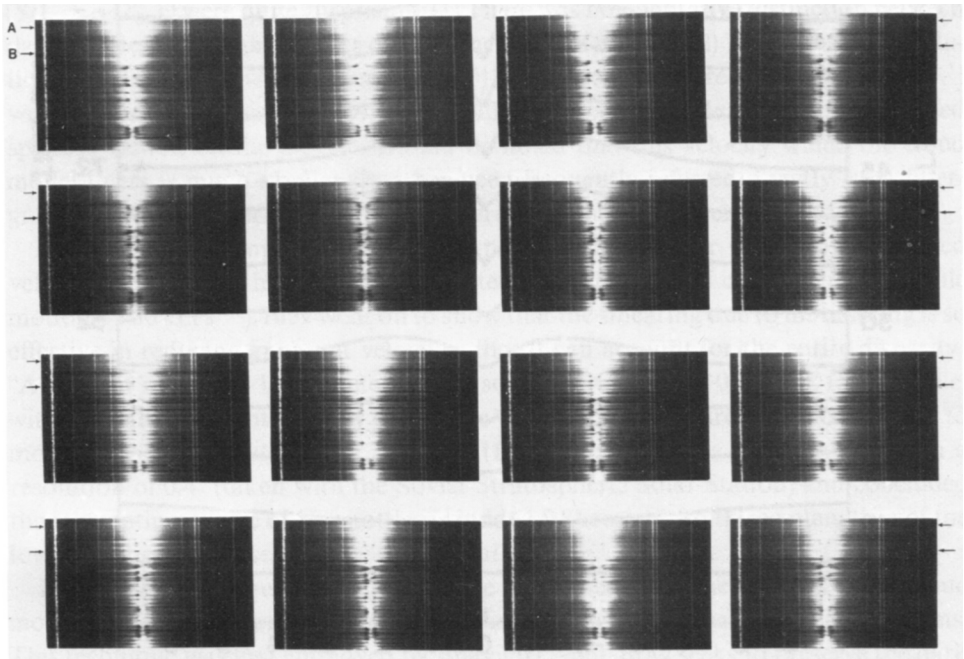


Fig. 8. A time sequence of K-line spectra of a quiet region at the center of the disk (from Liu, 1973). In this example  $\Delta t$  is 8 s between frames. The disturbance marked 'B' begins in the far  $K_1$  wing (first row), proceeds to the inner  $K_1$  wing (second row), produces an intense  $K_{2v}$  emission (third row) then fades out (fourth row).

### 3.4.1. Phenomenological Studies

Studies resulting from filtergrams, spectroheliograms, or direct attempts to interpret the  $H\alpha$  profile have had a long history. The benchmarks are perhaps the works of Bhavilai (1965) and Title (1966). Bhavilai inferred from  $H\alpha$  filtergrams that the mottles were moving downward close to the centers of the rosettes and were moving upward at greater distances from the rosettes. In many cases a connection between the two features was observed and loop-type motion was inferred.

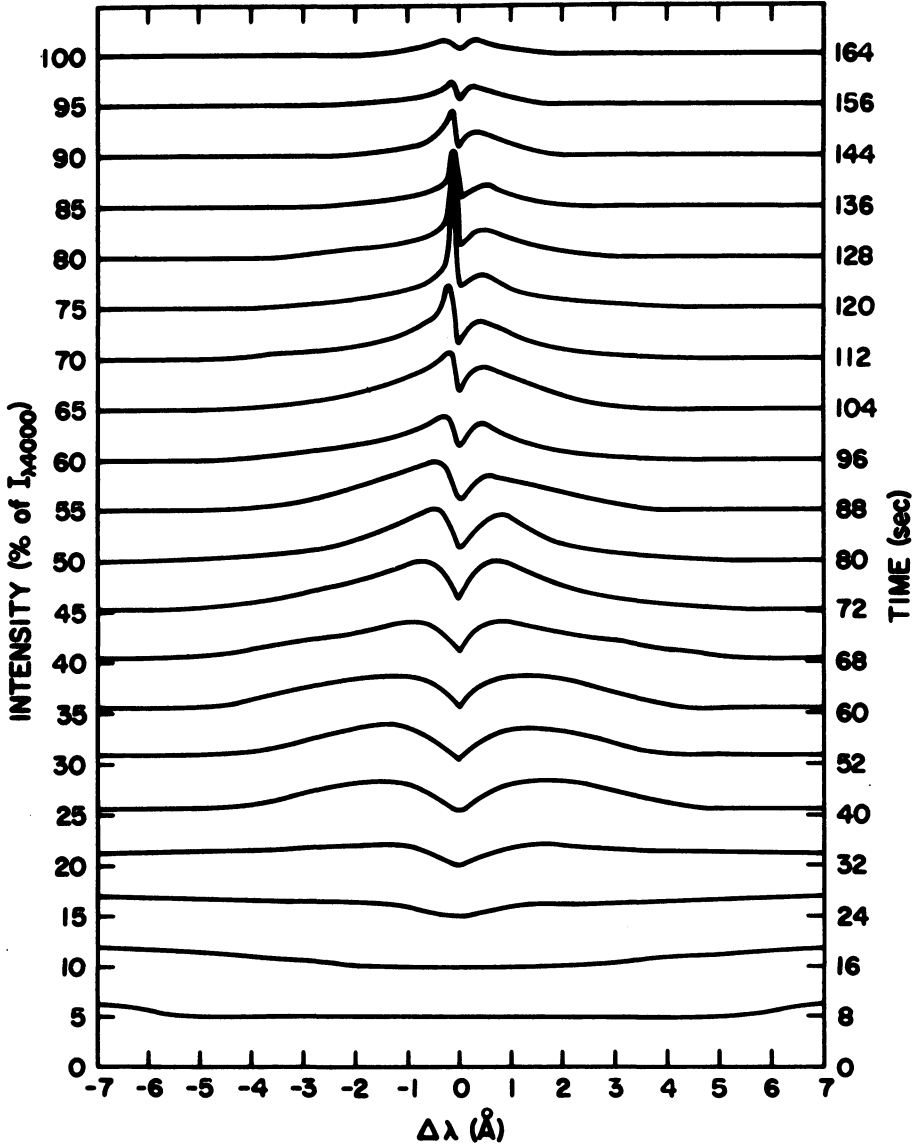


Fig. 9. Subtracted profiles (profile at time  $t$  minus profile at time 0) of event  $B$  of Figure 8 (from Liu, 1973).

Title confirmed the rough distribution of upflow and downflow elements, but found them to be completely different phenomena. Downflow elements were much longer-lived (6 to 9 min) than the upflow elements (2 min), and there was no correlation between the two features anyway. So this type of investigation has been left appropriately enough on a rather uncertain note.

#### 3.4.2. $H\alpha$ Profile Analyses

It was shown by Beckers (1962, 1964, 1968) and Athay (1970) that direct inference of velocities from  $H\alpha$  line shifts or asymmetries can lead to very inaccurate results. These ideas were tested and confirmed observationally in a pair of very important papers by Grossman-Doerth and von Uexküll (1971, 1973). Using data from simultaneous spectrograms and filtergrams, they tested both the 'cloud' model of Beckers and the 'velocity layer' model of Athay. The velocity layer model did not fit the mottle spectra, which is not surprising because it was so highly simplified (no variations in any of the other physical variables were allowed). However the cloud model fit the spectra very well, as shown in Figure 10. The cloud model assumes that a mottle is a separate cloud overlying the chromosphere. The physical variables are assumed to be constant throughout the cloud and the emitted profile is then fully determined by four quantities;  $S$ ,  $\tau_0$ ,  $\Delta\lambda_0$ ,  $v$ , the source function, the optical depth at line center of the cloud, the line width, and the bulk velocity, respectively.

The results of fitting these spectra to the four parameters of the cloud model ( $S/I_c$ ,  $\tau_0$ ,  $\Delta\lambda_0$ ,  $v$ ) were quite surprising: (1) There was no qualitative distinction between dark mottles and bright mottles or any other kind of mottles. (2) There was no correlation between any of the four parameters. (3) The velocities inferred (rms  $v = 3.6 \text{ km s}^{-1}$ ) were considerably smaller than what would be expected if  $H\alpha$  mottles were indeed spicules viewed on the disk. (It should be noted that this velocity which the cloud model infers is much smaller than has been frequently inferred directly from filtergrams. It is also larger than would be inferred by the line bisector method).

Recognizing the importance of the disparity between their rather low measured velocities and those that would be expected from the vertical component of spicule motion ( $\approx 30 \text{ km s}^{-1}$ ), they went on to show that the smearing due to finite seeing is so effective in reducing apparent velocities that it can account for the entire disparity; "A circular mottle of 1" diameter (and a seeing parameter of 0.7–1.5"), for example, with a true line of sight velocity of  $30 \text{ km s}^{-1}$  would in most circumstances appear to move with only about  $5 \text{ km s}^{-1}$ ". Krat (1972), measured  $H\alpha$  spectrograms with a resolution of 0.4" (taken with the Soviet Stratospheric Solar Station) and concluded that the optimum size of  $H\alpha$  mottles is indeed 0.8" to 1.1". So this explanation of the low velocities would seem to be a very realistic one.

Bray (1973) and Loughhead (1973) have performed the same analysis of the cloud model, using instead of spectrograms the interesting technique of tuned filtergrams. This technique was first employed by Bhavilai (1966). Bray seeks to preserve the dark mottle-bright mottle terminology; Loughhead seeks to show that the cloud model

breaks down near the limb. The point here is that, where velocities are concerned, Bray and Grossman-Doerth and von Uexküll are in agreement.

#### 4. Limb Phenomena

We now finally discuss spicules *per se*. At the very start, I must mention the excellent reviews by Beckers (1968, 1972), which I shall be using rather heavily. As an introduction a few words should be said as to how the size regimes mentioned in Section 2 are

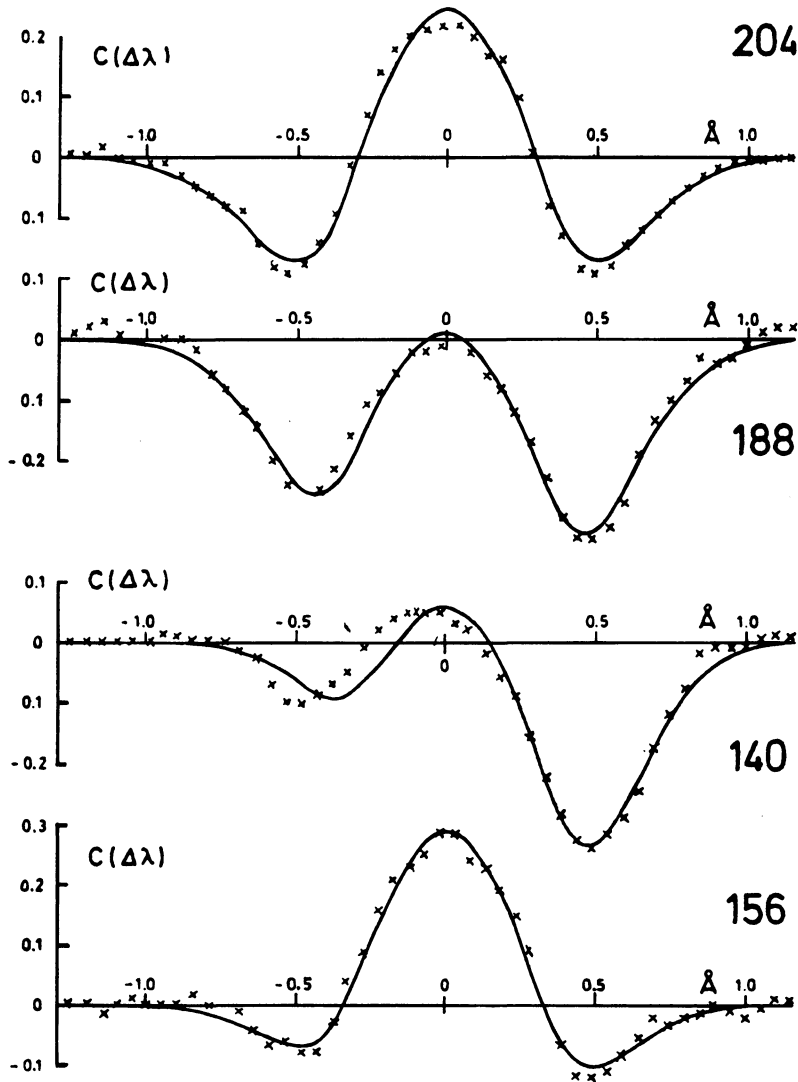


Fig. 10. Examples of contrast profiles  $C(\lambda) = (I - I_0)/I_0$  derived from  $H\alpha$  spectra (from Grossman-Doerth and von Uexküll, 1971). The crosses are the observed profiles, the solid lines are calculated profiles obtained by fitting Beckers' cloud model to the observations.

changed when applied to limb observations. Now all three spatial coordinates have separate effects, and any attempt to schematicize the regimes becomes three-dimensional and very complicated. Even more important, all the characteristic lengths are roughly the same as each other, *and roughly the same as the spicule diameters*. Furthermore, the optical depths of the spicules vary considerably with altitude and with the line observed. As a result, the interpretation of line shifts, widths, asymmetries, etc. in terms of detailed motions is on an even less sound basis than for disk features. Such terms as microturbulence or non-thermal motions should be used only in the broadest sense; they are little more than convenient terms to describe observable effects. It should also be noted that microturbulence occupies a unique position in that, as our understanding of the diagnostic problem worsens and as the observational data becomes more crude, a larger and larger fraction of the total motion is ascribed to microturbulence. Thus we can expect limb observations to imply larger values of microturbulence than disk observations. We should probably also expect large variations in all types of motions because the observable effects depend very strongly on instrumental parameters such as spatial resolution, height resolution, and even the spectral line observed.

#### 4.1. RESOLVED MASS MOTIONS

##### 4.1.1. *Proper Motions*

Almost all measurements of *vertical* proper motions were made in the 1950's and have been reviewed by de Jager (1959) and Beckers (1968). Most find a rise of about  $30 \text{ km s}^{-1}$  with occasional fast spicules. The time or height variation of spicule rises cannot be observed accurately enough to identify a particular type of trajectory, such as a rise at uniform velocity or a parabolic trajectory (Athay and Thomas, 1957), but there is a linear relation between maximum height attained and the velocity of ascent (Rush and Roberts, 1954). The fate of spicules after they reach maximum height however, is still uncertain. Lippincott (1957) observed roughly half of them to fall again; the other half simply fade away. In relation to this, Mouradian (1967) found spicules to diffuse at a rapid rate ( $10$  to  $20 \text{ km s}^{-1}$ ) while fading. Later measurements (Lynch *et al.*, 1973) contradict this. Since the later measurements were derived from the same observer using a better telescope, one must give greater weight to them and say that the diffusion of spicules is very much in doubt. Of course it is quite possible that spicules diffuse into the corona after they fade out and become invisible.

There are several recent reports of observed *horizontal* proper motions (Weart, 1970; Nikolsky, 1970; Pasachoff *et al.*, 1968; Nikolsky and Platova, 1971). One can easily imagine instrumental effects and particular spicule geometries that can create the appearance of horizontal proper motion, however all authors agree that the effect is definitely real. The observed speeds range from  $5 \text{ km s}^{-1}$  (the observational limit) up to  $60 \text{ km s}^{-1}$ . Nikolsky and Platova measure a distribution with a mean of roughly  $20 \text{ km s}^{-1}$  (Figure 11). They also observe the spicules to oscillate with a most probable period of  $\approx 1$  min. The observational constraints are such that this could also be

interpreted as random motion. It isn't clear *how many* spicules exhibit horizontal proper motion. We only know the number is more than 5% (Weart, 1970). It would be most valuable to get better statistics of this important phenomenon.

#### 4.1.2. Doppler Shifts

Most measurements of Doppler shifts have been reviewed by Beckers (1968). The rms velocities are about  $10 \text{ km s}^{-1}$ , while the maximum observed velocities are about

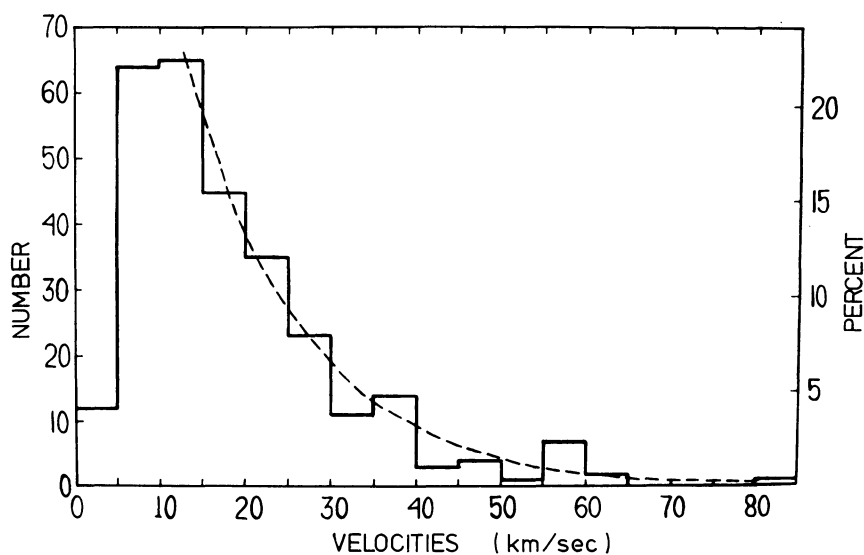


Fig. 11. The observed velocity distribution of transverse proper motions (from Nikolsky and Platova, 1971). The peak at about  $10 \text{ km s}^{-1}$  is probably caused by an observational cutoff at low velocities.

$30 \text{ km s}^{-1}$ . More recently, Krat and Krat (1971) observe significantly higher Doppler shifts. (They make a further startling observation; that Doppler shifts of spicules measured simultaneously in  $H\alpha$ , H & K, and  $D_3$  are not always the same. Table III lists the measured radial velocities of 15 spicules for which  $v_r$  was observed simultaneously in the  $H\alpha$ , K and  $D_3$  lines. Spicules Nos. 1 and 2 ( $h=7000 \text{ km}$ ) are the same spicules as Nos. 6 and 7 ( $h=8000 \text{ km}$ ) respectively. One can see many cases of large differences in  $v_r$ , between the three lines. We shall return to this point later.) The rms Doppler shifts, if interpreted as being caused by motion along the axis of the spicules, results in a mean axial velocity of the spicules of  $25$  to  $30 \text{ km s}^{-1}$  (Beckers, 1968).

There is contradictory evidence of the height variation of Doppler shifts. Mouradian (1965) finds a decrease with height, several others (Michard, 1959; Beckers, 1966) find an increase with height, and two groups Pasachoff *et al.*, 1968; and Nisolsky and Sazanov, 1966) find no significant change. It seems that the only tenable summary is that *on the average* there is very little height dependence, but that large fluctuations are possible. This is illustrated by the very wide scatter in Figure 12 (Pasachoff *et al.*, 1968). Here Doppler shifts at two different heights (simultaneous) are correlated.

TABLE III  
Radial velocity of 15 spicules measured simultaneously in three different lines  
(from Krat and Krat, 1971)

$h$ ( $10^3$ km)	Spicule No. <sup>a</sup>	$v_r$ ( $\text{km s}^{-1}$ )		
		H $\alpha$	Ca II K	D <sub>3</sub>
	1	0.0	0.0	0.0
	2	+5.0	+8.0	+5.0
7	4	0.0	0.0	0.0
	5	+2.3	0.0	-13.3
	6	+7.0	+5.0	+8.0
	7	+3.0	+9.0	+14.0
	8	-28.6	-17.2	-29.4
8	11	-27.7	-19.7	-
	12	+37.5	+21.9	-
	13	-28.0	-21.2	-29.4
6	15	+11.5	+6.9	0.0
	18	+10.7	+10.0	+2.5
	20	-31.8	-31.8	-31.5
7	22	+11.0	+8.0	+9.1
	23	0.0	0.0	0.0

<sup>a</sup> Spicules whose numbers do not appear did not have their radial velocities measured.

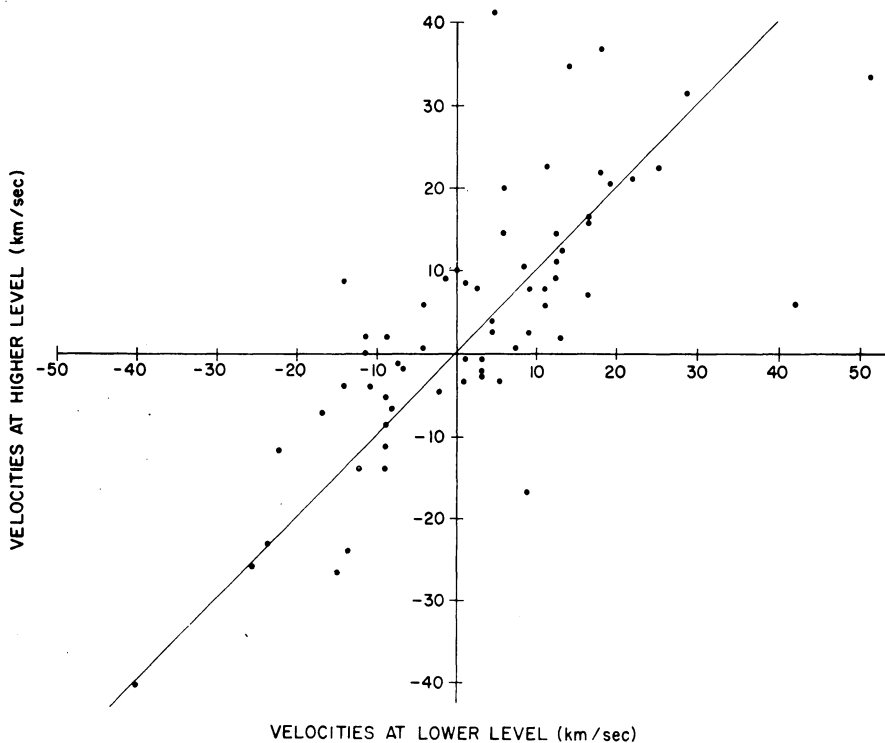


Fig. 12. Comparison of radial velocities measured simultaneously at two heights in H $\alpha$  (from Pasachoff *et al.*, 1968). The heights are separated by 1800 km. Positive signs indicate velocities of recession. On the average velocities are the same at the two heights, but the variations are large.

The time variation of Doppler shifts is also an open topic. Most authors seem to agree that the *majority* of features (perhaps 80%) exhibit a simple Doppler history of uniform rise or fall. Several observers (Nikolsky and Sazanov, 1966; Zirker, 1967; Pasachoff *et al.*, 1968) find features which reverse sign, oscillate, or otherwise show complicated behavior. Figure 13 (Pasachoff *et al.*, 1968) displays a good sample of

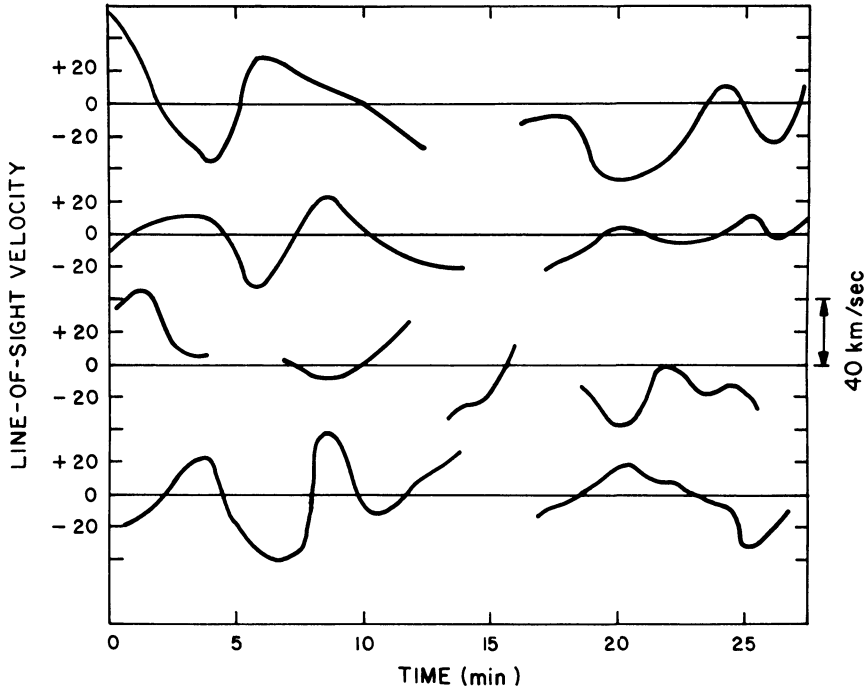


Fig. 13. Examples of spicules whose radial velocities vary significantly with time (from Pasachoff *et al.*, 1968).

such things. It is all very reminiscent of the observed horizontal proper motions mentioned earlier. In fact, Weart (1970) stated that the two are very closely coupled. In a number of cases, individual spicules showed complicated Doppler histories that were closely matched by simultaneous horizontal proper motions, indicating a transverse back and forth motion of the spicules along a direction inclined to the line of sight. Thus it seems that some unknown but probably small fraction of observed Doppler shifts must be interpreted as horizontal, not axial motion.

#### 4.1.3. Rotational Motions

Emission lines which are tilted slightly with respect to the direction of dispersion have been observed by many people (Michard, 1956; Livshitz, 1966; Pasachoff *et al.*, 1968; Weart, 1970). Such a tilted line can be seen in Figure 14 (Noyes, 1965). This is a very atypical example; most tilted line profiles are far less obvious. In fact in many cases,

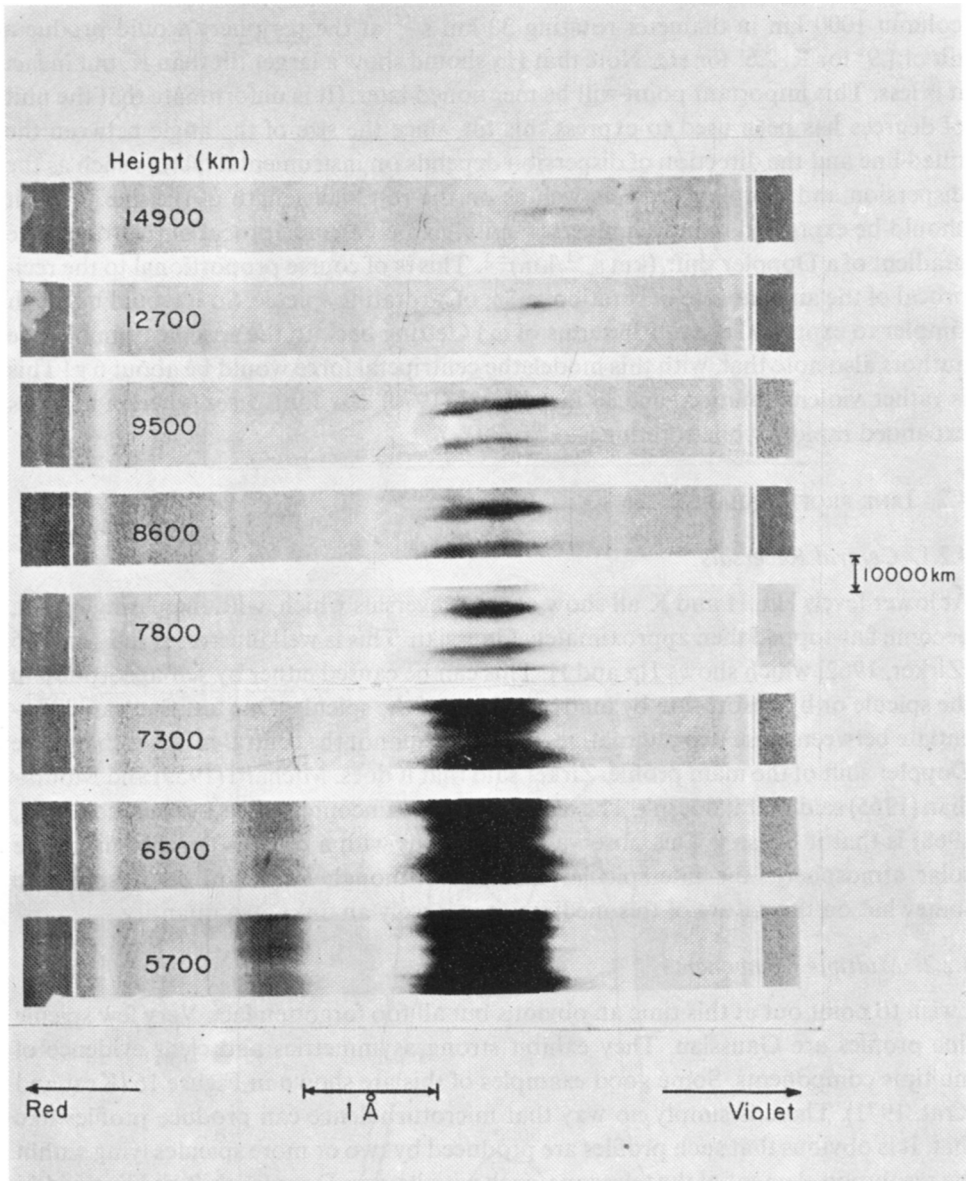


Fig. 14. The 'most outstanding example' of a tilted Ca II H line (from Noyes, 1965). The same feature is observed over a sequence of different heights. Note the apparent rapid increase of rotational speed with height.

the apparent tilt could be the result of two close, unresolved spicules, each with greatly different Doppler shifts. However, there are many cases where it seems clear that this tilt is real and results from spicule rotation (Beckers, 1966, 1968). But nobody says what *fraction* of spicules show tilted lines. The size of the tilts is small (e.g.  $\sim 2^\circ$  for K,  $\sim 1^\circ$  for H $\alpha$ , Pasachoff *et al.*) but quite important. Pasachoff *et al.* calculate that a

column 1000 km in diameter rotating  $30 \text{ km s}^{-1}$  at the periphery would produce a tilt of  $1.9^\circ$  for K,  $2.6^\circ$  for H $\alpha$ . Note that H $\alpha$  should show a larger tilt than K, but in fact it is less. This important point will be mentioned later. (It is unfortunate that the unit of degrees has been used to express this tilt, since the size of the angle between the tilted line and the direction of dispersion depends on instrumental factors such as the dispersion and the plate scale as well as on the rest wavelength of the line. The tilt should be expressed in more universal units; namely the reciprocal of the transverse gradient of a Doppler shift,  $(\text{km s}^{-1}/\text{km})^{-1}$ . This is of course proportional to the reciprocal of the angular rate of rotation,  $\omega^{-1}$ , of a rotating spicule. So it would be much simpler to express these tilts in terms of  $\omega$ .) Getting back to the specific example, the authors also note that, with this model, the centripetal force would be about 6 g! This is rather violent rotation, and in fact Weart (1970) saw four cases wherein spicules expanded rapidly while rotating.

## 4.2. LINE PROFILE SHAPES

### 4.2.1. *Central Reversals*

At lower levels H $\alpha$ , H and K all show central reversals which, with increasing height, become flat-topped then approximately Gaussian. This is well illustrated in Figure 15 (Zirker, 1962) which shows H $\alpha$  and H. This can be caused either by self-absorption in the spicule or by absorption by matter in front of the spicule. One test that can differentiate between these two alternatives is whether or not the central reversal shares the Doppler shift of the main profile. Zirker said that it does. Michard (1959) and Mouradian (1965) said that it doesn't. The latest and as yet uncontested vote (Pasachoff *et al.*, 1968) is that it doesn't. This observation leaves us with a curious component in the solar atmosphere: the interspicular medium. Although Pasachoff *et al.* speculate somewhat on the nature of this medium, it is largely an unknown quantity.

### 4.2.2. *Multiple Components*

I wish to point out at this time an obvious but all too forgotten fact. Very few spicule line profiles are Gaussian. They exhibit strong asymmetries and clear evidence of multiple components. Some good examples of this are shown in Figure 16 (Krat and Krat, 1971). There is simply no way that microturbulence can produce profiles like that. It is obvious that such profiles are produced by two or more spicules lying within the resolution element of the telescope, each with its own Doppler shift and line width. It is clear that the measurement of Doppler shifts and line widths of such profiles requires some care and judgment. One can measure the Doppler shift of the 'center of mass' of the entire profile and some sort of overall width. In this case the results will be abnormally low Doppler shifts and large widths. Alternatively, one could try to identify the individual components and measure them separately. This procedure is more realistic, but is also tedious and requires some subjective judgment. Both approaches can be found in the literature, which makes comparison of published values difficult. Some authors don't even confide which approach they used.

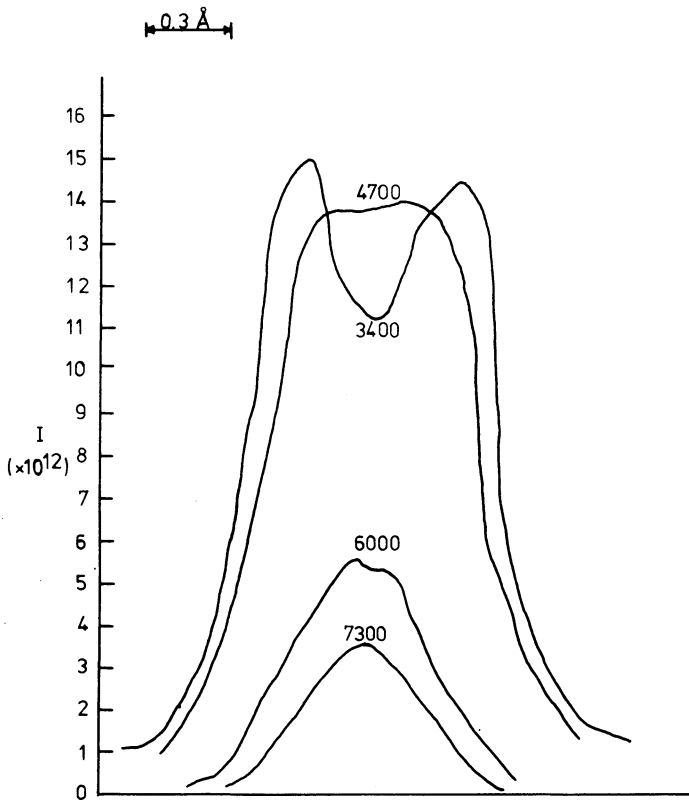
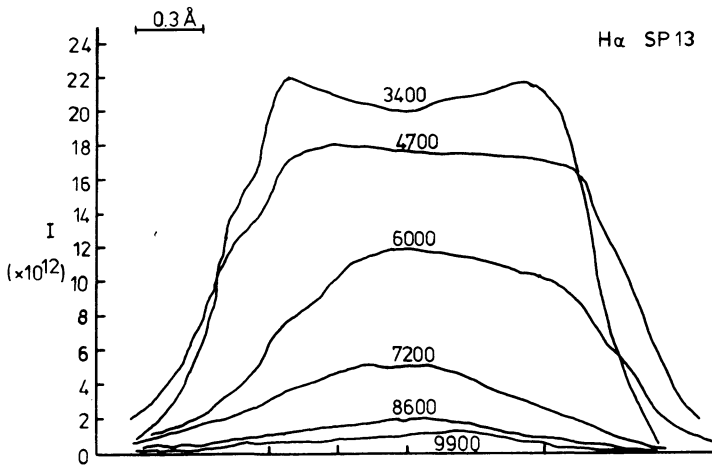


Fig. 15. Typical profiles of H $\alpha$  and Ca II H at different heights (from Zirker, 1962).

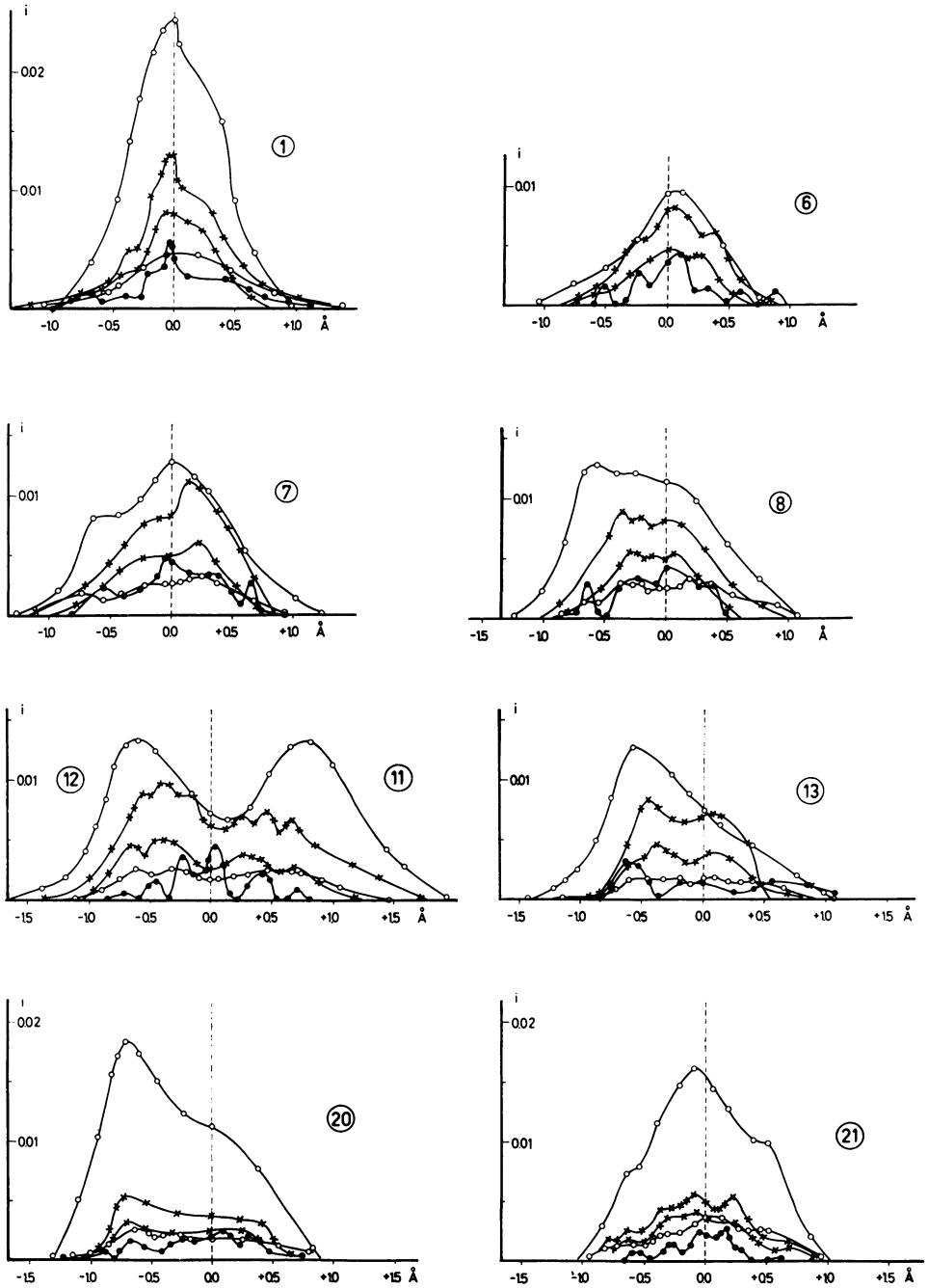


Fig. 16. Outstanding examples of spicule profiles with multiple components (from Krat and Krat, 1971). These were selected as being 'narrow faint line profiles'. Open circles are  $H\alpha$  and  $H\beta$ ,  $\times$ 's are H and K, filled circles are  $D_3$ .

### 4.3. LINE WIDTHS

In this section we will consider the variation of line widths first as a function of  $\mu$ , (the mean atomic weight), then as a function of height. There are two ways to consider this variation; statistically (e.g. the average H $\alpha$  width versus the average K width), and individually (i.e. simultaneous measurements of both lines in an individual spicule). In both cases we will consider the statistical method first and the individual method second. We will also adopt Beckers' notation for line widths;  $W = \Delta\lambda_2/\lambda$ , where  $\Delta\lambda_2$  is the full width at half maximum of an emission line.

There has been essentially no work done on this topic since the reviews by Beckers. This is in itself an important and surprising point. Where have all the observers gone, these last two years?

#### 4.3.1. The Variations of $W$ with $\mu$

Following Beckers, we expect  $W$  to be composed of two parts; the thermal part and the non-thermal part. The thermal part varies as  $\mu^{-1/2}$ ; the non-thermal part is a constant. So they should sum together as follows:

$$W^2 = W_{nt}^2 + W_t^2/\mu. \quad (3)$$

Figure 17 is a plot of  $W^2(\mu^{-1})$  from Beckers (1968). One should be able to fit a straight

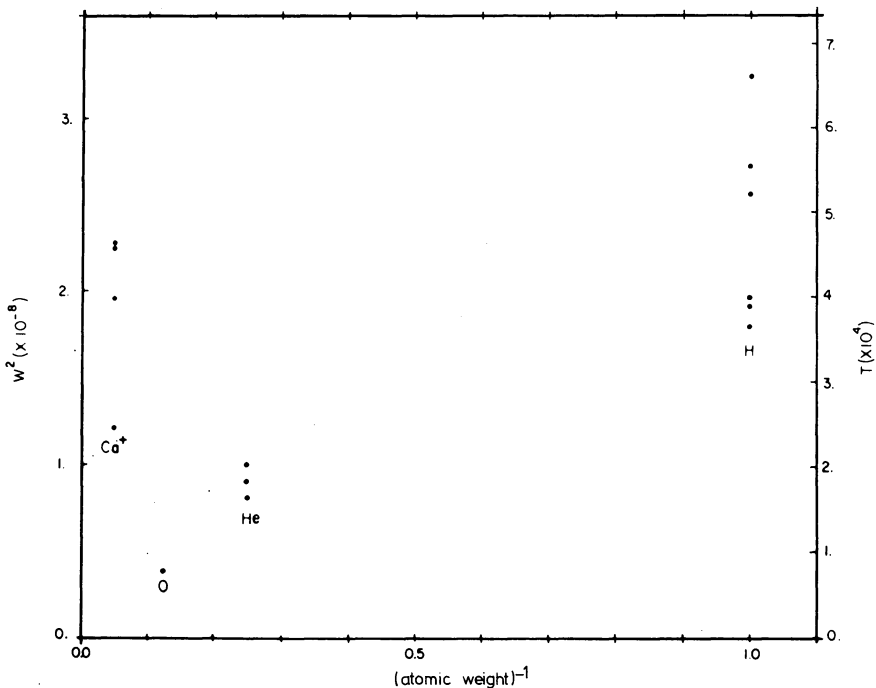


Fig. 17. Dependence of the half-widths of hydrogen, helium, oxygen, and ionized calcium emission lines in spicules on the atomic weight (from Beckers, 1968). The temperature scale on the right is for hydrogen atoms assuming the line width to be entirely thermal. The points represent the most likely value of  $W^2$  for each observed line.

line to these data, the intercept yielding  $W_{nt}^2$ . One can see the problem. Actually, the situation is worse than this, because Beckers had already averaged many points so that each point on Figure 17 represents an average value of all measurements of a single line. (The widths are measured at about 3000 to 6000 km above the limb.) All the published values of  $W$  yield Figure 18. It is obvious that H and Ca display enor-

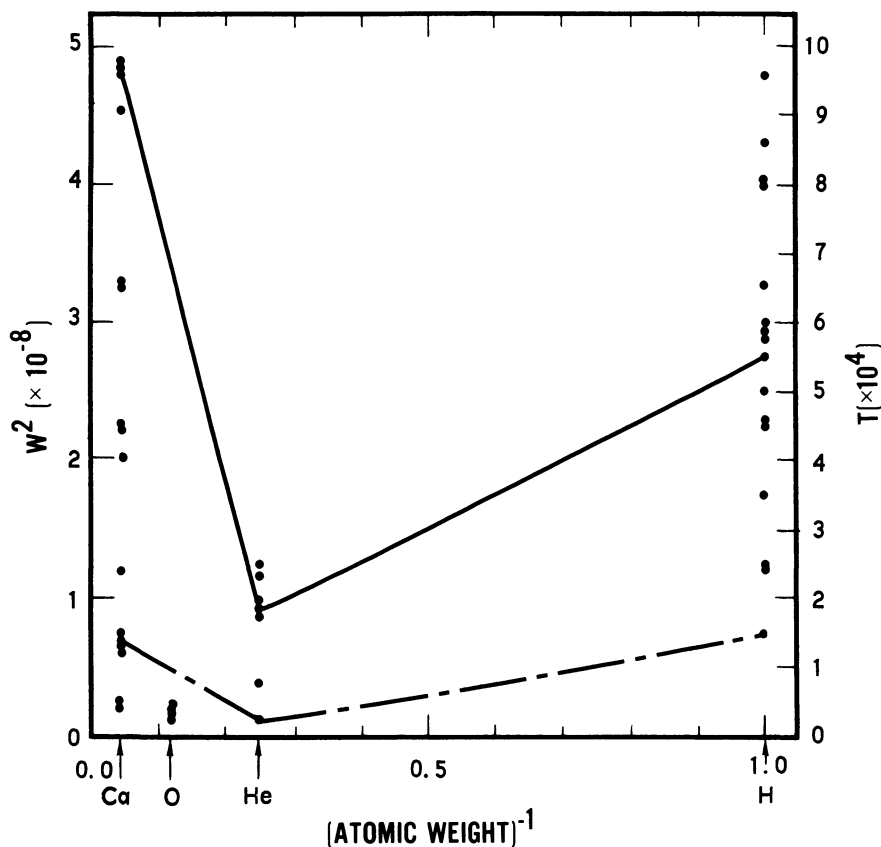


Fig. 18. Identical to Figure 17, but with all published values of  $W^2$  plotted. Note the wide variations of  $W$  for hydrogen and calcium. Solid line, average  $W^2$  (for  $H\alpha$ ,  $D_3$  and  $K$ ) of wide line spicules; Dashed line,  $W^2$  of narrow line spicules (data from Krat and Krat, 1971).

mous variations, which led Athay and Bessey (1964), Beckers (1968, 1972) and Krat and Krat (1971) to speak of 'wide line spicules' and 'narrow line spicules' as if they were two different types. There is however no evidence that there is not a continuous distribution of  $W$ .

Now, one can conclude either that the calcium lines are anomalously broad (and  $T_e$  is high,  $\xi_r$  low) or that the helium and oxygen lines are anomalously narrow (and  $T_e$  is low,  $\xi_r$  high), or that the different lines are formed in different regions with different  $T_e$ 's and  $\xi_r$ 's.

#### 4.3.2. *Observational Sources of Variations*

Before proceeding, I would like to stop for just a moment and list very briefly possible observational sources of these wide variations:

(1) Resolution (both seeing and instrumental). We know from Section 4.2.2 that finite resolution has a strong effect on  $W$ , but it is very difficult to evaluate.

(2) Are we even looking at the same spicules in the different lines? Faint lines may be formed preferentially lower; strong lines may be formed higher, or even only in foreground spicules. Pasachoff *et al.* (1968) claim to rule out this effect, but their data is open to debate.

(3) The faint lines are very sensitive to scattered light and even to effects of under-exposure. I note that the oxygen lines are too faint even to allow the measurement of individual spicules.

(4) Since the range of wavelengths is great, there is a strong possibility of chromatic effects (differential seeing, chromatic aberrations, etc.)

(5) The methods of measuring  $W$  vary from observer to observer as mentioned earlier. For example, Athay (1961) seemed to measure a composite width, while Krat and Krat tried to separate various components of a profile.

#### 4.3.3. *Simultaneous Observations of Different Lines*

The advantages of simultaneous observations are obvious. Krat and Krat (1961) compared  $H\alpha$  and  $D_3$ , Gulyaev (1965) and Nikolskaya (1967) compared  $H_8$  and  $HeI \lambda 3889$ ; Pasachoff *et al.* (1968) compared various combinations of H, K,  $He$ ,  $D_3$  and the Ca II IR triplet, but reported no width measurements. The most comprehensive work has been that of Krat and Krat (1971) who observed  $H\alpha$ ,  $H\beta$ , H, K, and  $D_3$  simultaneously. All these observations essentially confirm our impressions from Figure 18; compared to  $H\alpha$ ,  $D_3$  is so narrow as to imply almost no non-thermal velocities, and Ca is so wide as to imply huge velocities. A warning should be noted however when comparing lines of different strengths, as mentioned earlier in Section 4.3.2, item No. 2. In this case,  $D_3$  is much fainter than  $H\alpha$ ,  $H\beta$ , H or K, so one should be cautious when interpreting differences between  $D_3$  and these other lines.

#### 4.3.4. *Height Variations of $W$*

It has been mentioned by nearly everyone who has analyzed spicule spectra that the broad profiles may be caused by unresolved clumps of spicules, each with their own Doppler shift. It has been stated often that this effect can be tested by seeing if a broad profile of a particular spicule breaks up into several resolved narrower profiles at higher altitude, where the spicule count is lower and the spicules are more likely to be resolved. This is not really a valid test, since most components of a composite profile would simply fade out with altitude, not separate spatially. One can only measure  $W(h)$ .

Measured statistically,  $W(h)$  does decrease for hydrogen and calcium and increase for helium. All observers agree at least on the sign but disagree on the magnitude. Some of the largest height changes were measured by Zirker (1963), Figure 19.

Measured *individually*, the situation is much different. Athay and Bessey, for example, state that profiles of individual spicules do not change with height; that the statistically observed decrease of  $W$  with  $h$  is caused by the fact that the relative population of narrow line profile is greater at high altitudes (i.e. narrow line spicules are *taller* than broad line spicules). This is in fact the origin of the two 'types' of

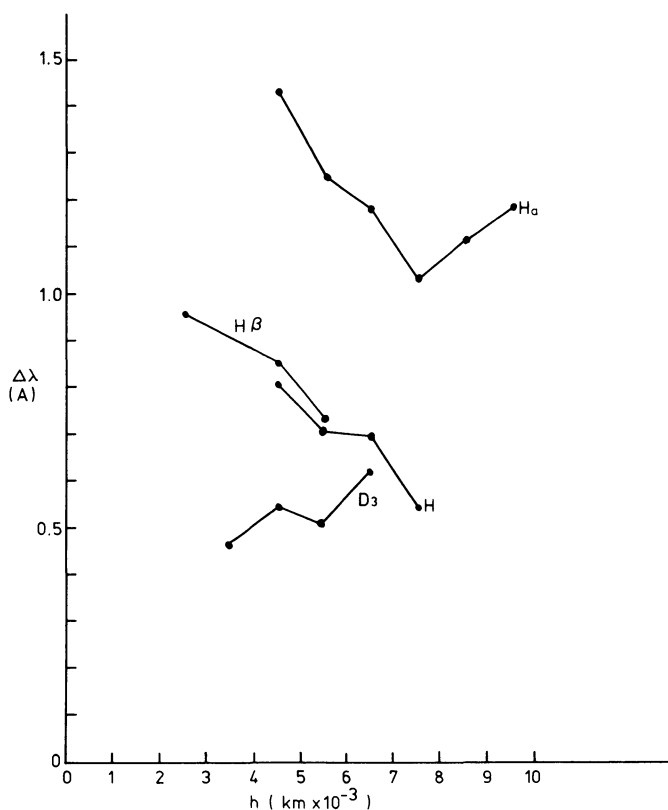


Fig. 19. The height variation of the *average* half-widths (in ångströms) of spicule line profiles (from Zirker, 1962). Other average measurements show less dependence on  $h$ .

spicules. This point seems to be quite a source of argument. Pasachoff *et al.* (1968) have joined Athay and Bessey, while Zirker (1962), Gulyaev and Livshitz (1966) and Giovanelli *et al.* (1965) argue the opposite.

Actually the question of whether or not the broad line profiles come from unresolved clumps of spicules becomes somewhat academic if it is used as an explanation for the anomalously broad calcium lines. The reason for this is that, although one can find individual spicules with rather narrow calcium lines, those same spicules also have narrow hydrogen lines. This point was mentioned by Athay and Bessey, and shown rather clearly by Krat and Krat (1971). They measured the widths of 'wide line' spicules and 'narrow line' spicules for  $H\alpha$ ,  $H\beta$ , K, H and  $D_3$  (Table IV).

Although it is still not clear whether the wide line spicules are unresolved clumps of spicules or have their lines intrinsically broadened, it is clear that in the narrow line spicules, *all* the lines are narrow (in fact  $D_3$  is so narrow as to put severe upper limits on  $T_e$  and/or  $\xi_r$ .) Thus, no matter which type of spicule one chooses as being 'the

TABLE IV  
Mean widths of line profiles of spicules (after Krat and Krat, 1971)

Profile Characteristic	Line	H $\alpha$	H $\beta$	K	H	D $_3$
Narrow	No. of spicules	6	4	5	6	20
	$W (\times 10^{-4})$	0.87	1.11	0.84	0.82	0.32
Wide	No. of spicules	3	3	3	3	3
	$W (\times 10^{-4})$	1.68	2.08	2.19	2.14	0.97

real spicule', the  $W^2(\mu^{-1})$  function remains non-linear. This can be seen on Figure 18, where Krat and Krat's data for the two types of spicules are shown.

#### 4.4. SUMMARY AND INTERPRETATIONS

It is time to collect all the data mentioned in this section and attempt to combine it into a cohesive empirical model. First a few editorial comments are probably in order. The one thing that is clear from all this data is that spicules possess huge variations. It is also clear that observers possess an amazing proclivity for observational selection. These two points together spell danger and demand caution in any interpretation. Of course, the problem of observational selection is an unavoidable result of the spectrographic technique. Spicule spectra preferentially show spicules which are unusually bright, tall, more isolated or have larger Doppler shifts than the 'typical' spicule. But this only means that observers should be doubly careful to obtain a statistically meaningful sample of spicule spectra. And anyone who interprets such spectra should understand that he might be describing or explaining a very atypical spicule. A separate point is that, in contrast to the preceding section on disk phenomena, here there seems to be a clear need for more and better observations. Such observations are well within present capabilities; they will be mentioned in detail below.

##### 4.4.1. Mass Motions

The picture which seemed rather clear a few years ago has now become if anything, a little more confused. The correspondence between proper motions and Doppler shifts in terms of axial motion of inclined spicules should be generalized somewhat to include the increased values of the Doppler shift and the observed horizontal motions. However, an improved empirical model of these motions is not possible at

the present time due to the lack of detailed data. Furthermore, the observed diffusion of spicules into the corona is now in doubt. So the fate of the half of the spicules which are not observed to descend again is still an open question. The classical description of a spicule as rising along its axis at about  $30 \text{ km s}^{-1}$ , then either descending back down the same path or diffusing and descending somewhere else seems to remain reasonably valid as an average scenario. But there are significant uncertainties as to variations from this mean behavior which can and should be answered observationally. The tool to use is a time sequence of spectrograms combined with simultaneous entrance slit filtergrams.

#### 4.4.2. *Internal Motions*

Interpretation in terms of internal motions centers on the explanation of the large widths of the spectral lines. There are two general possibilities: (1) the spicules are unresolved, and each spicule displays a different radial velocity,  $v_r$ . (2) the spicules possess structure, that is different lines are formed in different regions of the spicule, with different values of  $T_e$ ,  $\xi$ , and perhaps  $v_r$ . The most important point to make concerning these two possibilities is that they are not mutually exclusive. In fact, there is quite valid evidence which virtually demands that each possibility at least partially accounts for the line widths.

The first possibility has already been discussed in Section 4.3.4. To that discussion should be added two results from broad-band measurements. The measured diameters of spicules are about 900 km (Lynch, *et al.*, 1973; Dunn, 1960, 1965). This diameter is slightly less than the resolution of most spectrographs. Also, at least in H $\alpha$  below 5000 km, there must be overlapping of spicules because spicule counts actually decrease in that region (Athay, 1959). So we must assume that all strong lines show effects of unresolved clumps of spicules below at least 5000 km. The composite profiles discussed in Section 4.2.2 confirm this. It has been argued (Athay and Bessey, 1964) that this effect cannot be the principal explanation for the large widths because then a decrease in widths would be accompanied by an increase in radial velocities of up to  $30 \text{ km s}^{-1}$ , and this was not observed. However these authors did detect at least a tendency for narrow widths to be correlated with large radial velocities, so this effect must be of secondary importance. The variation of line width with height furnishes evidence that is only inconclusive. The simultaneous measurements of Krat and Krat (Section 4.3.4) however furnishes conclusive evidence that lack of resolution will never explain the anomalous variation of line widths with atomic weight. So we can make two conclusions concerning this possibility of 'smearing broadening'; (1) Smearing does definitely artificially increase the widths of all lines by some as yet unknown amount. (2) Smearing broadening cannot account for the observed strange  $W^2(\mu^{-1})$  behavior.

There is evidence for the second possibility of structured spicules in addition to a simple lack of an explanation of the  $W^2(\mu^{-1})$  plot. First, the observation by Krat and Krat that some spicules show different radial velocities in different lines (Section 4.2.2). Further, the same authors note that D<sub>3</sub> spicules are more diffuse than H $\alpha$

spicules and that “there appears considerable interspicular emission (in  $D_3$ ) sometimes nearly of the same intensity as the emission in spicules”. There is supporting evidence, although weaker, from Pasachoff *et al.* (1968). The cross correlation between the brightness in  $D_3$  and in a wing of H or K is only 0.3. Even the correlation between H $\epsilon$  and H or K is only 0.6. Of course some part of the decrease in correlation is caused by differences in line strength, but still the correlations are rather low. The authors’ own conclusions from this data should be noted; “A given spicule emits simultaneously in lines of hydrogen, helium and calcium. This does not mean that the emission comes from the same volume within that spicule.” In summary, several different pieces of evidence seem to demand the conclusion that spicules are usually structured somehow, but lack of more detailed data prevents a specific model.

One of the simplest possible models is that of a spinning spicule, which has been investigated by Rodionov (1968) and Avery (1970). The hydrogen and helium lines fit a rotational velocity of 19–23 km s<sup>-1</sup> (Rodionov); the calcium lines require 22–36 km s<sup>-1</sup> (Avery). These calculations should be checked however not by line widths, but by line tilts (which measure  $\omega^{-1}$ ) of different lines *simultaneously*. The really important aspect of the structured model is that different lines must be formed in different regions, and there is not yet any direct evidence that demands this. Line tilts could be that evidence. Remember that, in the one specific observed example discussed in print, the tilts of the H $\alpha$  and the K line did not agree with each other if one were to assume a homogeneous spicule.

If we accept the fact that both ‘rotation broadening’ and ‘smearing broadening’ are at work simultaneously, we can to some extent understand the disparate observations of line widths and their height variation. Both broadening mechanisms will have distribution functions independent of each other, and both will be different functions of height. As a result of all the different possible combinations, we can expect to see a wide variety of phenomena. Broad lines could come from either rapidly rotating spicules *or* unresolved spicules and thus should be common. Narrow line spicules must be slowly rotating *and* well-resolved and thus rare. Lines which are narrow down low will stay narrow at greater heights. Lines which are broad down low could either remain broad at greater heights (due to a constant rotation) or become narrower (due to decreased smearing). All of this has been observed. The introduction of more complicated inhomogeneities or differential velocities, such as very narrow cores, sheaths, knots, etc. is of course a possibility and represents yet another level of complexity. At the present, this subject is a total unknown, both theoretically and observationally.

#### 4.4.3. *Approximate Numerical Values*

Three basic different types of motion have been observed, all of which may or may not be lumped together as ‘non-thermal’ motion: radial velocity,  $v_r$ , rotational velocity,  $v_{rot}$ , and microturbulence,  $\xi_r$ . Each of these types of motion can vary from spicule to spicule independently. So it is not surprising to find widely differing values quoted in the literature. Any attempt to summarize actual values of these three types of motions necessarily requires a large degree of judgment (i.e. guesswork) and should

include an indication of the range of variation that is possible from spicule to spicule. These are the current 'best guesses'.

$$\begin{aligned}v_r &\approx 15 \pm 10 \text{ km s}^{-1} \\v_{\text{rot}} &\approx 20 \pm 10 \text{ km s}^{-1} \\ \zeta_t &\approx 7 \pm 7 \text{ km s}^{-1}\end{aligned}$$

They all have large intrinsic dispersions. Note that there is no compelling evidence for supersonic microturbulence, but it is probable that mass motions are supersonic.

#### 4.4.4. *Further Observations*

Due to the oft-mentioned wide variations, statistical analyses do not seem to be as powerful as analyses of individual spicules. But the 'individual' method *must* be made more comprehensive. More lines, particularly oxygen, must be observed simultaneously. For example, if someone were to observe H $\alpha$ , D $_3$ , the Ca IR triplet, the O triplet, and perhaps 10830 simultaneously, he could probably rewrite the book. Also, different heights should be observed simultaneously. This can be done with image slicers. Lastly, line tilts of the different lines should be observed simultaneously. This is very difficult, but there are certainly some secrets there, waiting to be discovered.

## 5. Comparison of Limb and Disk Phenomena

At this point it would be nice if one could combine limb and disk observations of fine structure motions into a single model. Unfortunately, this is not possible. In fact, I am troubled by several very large discrepancies between limb and disk observations. One can only hope that these discrepancies are not fundamental, but are rather a result of insufficient data. Thus, my purpose in this section will be to point out several of the important pieces of the puzzle that are conspicuous by their absence, and to suggest research which could possibly supply those missing pieces.

### 5.1. FLOW PATTERNS

One would hope that, through the study of resolved motions as a function of space and time, one could deduce flow patterns that would at least statistically result in a single model for limb and disk features. This is a classic puzzle problem, and there are too many pieces missing to proceed. On the disk, the profile-blind technique of Bhavilai and Title established the existence and spatial relationship of upflows and downflows, but left the connection between the two literally up in the air. The high resolution profile work of Grossman-Doerth and von Uexküll proved much better at measuring velocities, but did not address itself to the spatial relationships. Such work is sorely needed, and the 'tuned filtergram' technique is a perfect tool for this purpose.

On the limb, the question of the reality of apparent proper motions must really

be considered open. The same can perhaps be said of the question as to what fraction of the observed Doppler shifts is due to axial motion and what fraction is due to horizontal motion. These questions can be addressed by some good solid analysis of tuned filtergram movies, for example, or time sequences of spectrograms combined with entrance slit filtergram movies. Furthermore, I note the fact that no one has really analyzed the horizontal motions of disk features. This is an obvious piece of work that should be done.

## 5.2. LINE PROFILES

### 5.2.1. *The Question of Velocities and Widths*

Both the velocities and line widths of H $\alpha$  mottles on the disk, as measured by Bray and by Grossman-Doerth and von Uexküll, are considerably smaller than those seen on limb spectra. In fact, the measured widths on the disk,  $W \approx 0.8 \times 10^{-4}$ , agree with Beckers' spicule model, which has no non-thermal motions *at all!* Perhaps we should be thankful that we finally have a case where observed widths agree with computed widths without resorting to non-thermal motions, but I am troubled by it because neither case agrees with limb observations.

The disk velocities are almost an order of magnitude lower than the limb velocities. Grossman-Doerth and von Uexküll showed that this could be caused by seeing effects, i.e. loss of resolution. But, if this were the case, then the line widths should be correspondingly large, since an increased line width is the classic symptom of unresolved mass motion. But, as we have mentioned, the line widths are too small, not too large. So if the H $\alpha$  mottles are deconvolved to achieve higher velocities, the widths would become smaller still and probably would even set severe upper limits on  $T_e$ . Unfortunately, this point was not investigated. It should be.

There exists an interesting possibility that the small disk widths and large limb widths imply that the unresolved mass motions in spicules are largely horizontal, as in rotational motion, or helical motion with a small pitch angle for example. This idea is however pure speculation at this time.

### 5.2.2. *Profiles near the Limb*

When confronted with a discrepancy, as in the line widths, between the disk and the limb, the logical place to look for an answer is in between; near the limb. Loughhead (1973) did exactly that and found that the H $\alpha$  profiles showed characteristics very similar to spicule profiles; large widths, central reversals and asymmetries. Figure 20 shows contrast profiles of dark mottles at  $\theta = 79^\circ$ , and they are starting to look very much like spicules. The widths are so broad that Loughhead couldn't even measure them. The central reversals violate the cloud model, as do the spicules. It is clear that a more sophisticated model than the cloud model is needed to provide the framework within which to analyze these mottle profiles. (And of course observations over a wide range of  $\theta$  are also needed). However, if this could be accomplished it is obvious that this topic will be an extremely fruitful field of work.

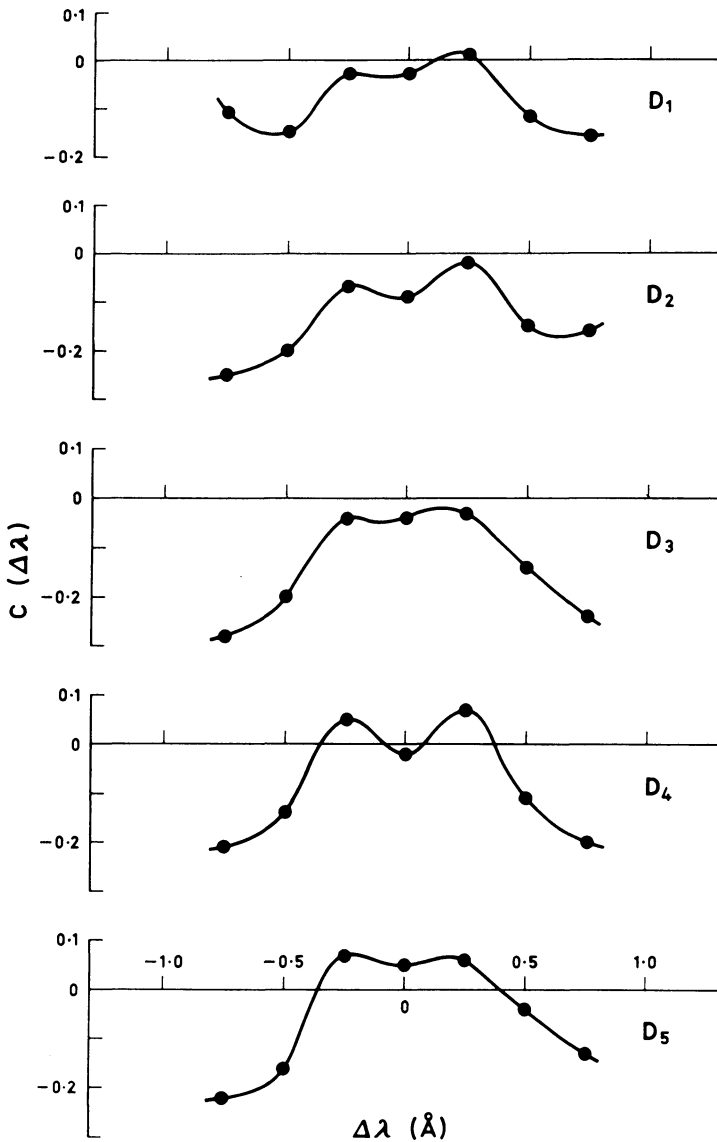


Fig. 20. Contrast profiles of dark mottles measured at  $\theta = 79^\circ$  (from Loughhead, 1973). The profiles exhibit central reversals, suggestive of spicules. The maximum contrast occurs beyond  $\frac{1}{4}$  Å, the tuning limit of the filter.

### 5.3. SUMMARY

There remains one last point of substance to be made. Lurking beneath the entire discussion of this last section is the question that when we compare disk and limb

observations, are we really looking at the same features at all? It is perhaps appropriate to end this review on a negative note by pointing out the following possibility: On the disk we are looking at features which lie below about 4000 km and which are relatively highly inclined, whereas the features we see on limb spectra are primarily above 4000 km, are more vertical, move faster, and have larger internal motions. We don't see the high features on the disk because they are too thin optically; we don't see the low features on the limb because they are too crowded to be resolved.

Certainly such a situation would explain why we have such difficulty identifying spicules on the disk. There is actually only one strong argument against this idea: In spicule models (cf. Beckers, 1972) spicules are indeed optically thick in the strong lines, and that is perpendicular to their long axis. On the disk, one would be looking at an acute angle to the spicule axis, hence through a longer path length through the spicule. Thus the spicule would be optically even thicker and should be visible on the disk. Playing the devil's advocate though, one should point out that this argument is model dependent, and one must wonder how sensitive the predicted optical depth of a spicule is to reasonable changes in the model. Further, there is a possible geometrical rebuttal; perhaps spicules are actually much narrower than observed. Then their contribution to a spectrographic resolution element on the disk could be very small and easily overwhelmed by the underlying chromosphere.

This question is of course an open one and probably will remain so until we fully understand the profiles of H $\alpha$  mottles as a function of  $\theta$ . It is at least comforting to know that there is plenty of research yet to be done.

## References

- Athay, R. G.: 1959, *Astrophys. J.* **129**, 164.  
 Athay, R. G.: 1961, *Astrophys. J.* **134**, 756.  
 Athay, R. G.: 1970a, *Solar Phys.* **11**, 347.  
 Athay, R. G.: 1970b, *Solar Phys.* **12**, 175.  
 Athay, R. G. and Bessey, R. J.: 1964, *Astrophys. J.* **140**, 1174.  
 Athay, R. G. and Canfield, R. C.: 1969, in Groth and Wellman (eds.), 'Spectrum Formation in Stars with Steady State Extended Atmospheres', *U.S. NBS Special Report No. 332* (IAU Colloquium No. 2), p. 65.  
 Athay, R. G. and Moreton, G. E.: 1961, *Astrophys. J.* **131**, 935.  
 Athay, R. G. and Thomas, R. N.: 1957, *Astrophys. J.* **125**, 806.  
 Avery, L. W.: 1970, *Solar Phys.* **13**, 301.  
 Bappu, M. K. V. and Sivaraman, K. R.: 1971, *Solar Phys.* **17**, 316.  
 Beckers, J. M.: 1962, *Australian J. Phys.* **15**, 327.  
 Beckers, J. M.: 1964, Thesis, Utrecht.  
 Beckers, J. M.: 1966, in K. O. Kiepenheuer (ed.), *The Fine Structure of the Solar Atmosphere*, Franz Steiner Verlag, Wiesbaden.  
 Beckers, J. M.: 1968, *Solar Phys.* **3**, 367.  
 Beckers, J. M.: 1972, *Ann. Rev. Astron. Astrophys.* **10**, 73.  
 Beebe, H. A.: 1971, *Solar Phys.* **17**, 304.  
 Beebe, H. A. and Johnson, H. R.: 1969, *Solar Phys.* **10**, 79.  
 Bhavilai, R.: 1965, *Monthly Notices Royal Astron. Soc.* **130**, 411.  
 Bhavilai, R.: 1966, in K. O. Kiepenheuer (ed.), *The Fine Structure of the Solar Atmosphere*, Franz Steiner Verlag, Wiesbaden.

- Bray, R. J.: 1973, *Solar Phys.* **29**, 317.
- Canfield, R. C.: 1969, *Astrophys. J.* **157**, 425.
- Canfield, R. C.: 1971, *Solar Phys.* **20**, 275.
- Cannon, C. J.: 1971, *Solar Phys.* **16**, 314.
- Cannon, C. J.: 1971, *Solar Phys.* **21**, 82.
- Cannon, C. J. and Rees, D. E.: 1971, *Astrophys. J.* **169**, 157.
- Cram, L. E.: 1972, *Solar Phys.* **22**, 375.
- de Jager, C.: 1959, *Handbuch der Physik* **LII**, 80.
- Dunn, R. B.: 1960, Thesis, Harvard.
- Dunn, R. B.: 1965, *AFCRL Env. Res. Paper*, No. 109.
- Giovanelli, R. G., Michard, R., and Mouradian, Z.: 1965, *Ann. Astrophys.* **28**, 871.
- Grossman-Doerth, U. and von Uexküll, M.: 1971, *Solar Phys.* **20**, 31.
- Grossman-Doerth, U. and von Uexküll, M.: 1973, *Solar Phys.* **28**, 319.
- Gulyaev, R. A.: 1965, *Soln. Dann.* **6**, 51.
- Gulyaev, R. A. and Livshitz, M. A.: 1965, *Astron. Zh.* **42**, 584.
- Jones, R. A. and Rense, W. A.: 1970, *Solar Phys.* **15**, 317.
- Krat, V. A.: 1972, *Solar Phys.* **27**, 39.
- Krat, V. A. and Krat, T. V.: 1961, *Izv. Pulkova* **22**, No. 167, 6.
- Krat, V. A. and Krat, T. V.: 1971, *Solar Phys.* **17**, 355.
- Kulander, J. L.: 1967, *Astrophys. J.* **147**, 1063.
- Kulander, J. L.: 1968, *J. Quant. Spectr. Radiative Transfer* **8**, 273.
- Kulander, J. L. and Jeffries, J. T.: 1966, *Astrophys. J.* **146**, 194.
- Leighton, R. B., Noyes, R. W., and Simon, G. W.: 1962, *Astrophys. J.* **135**, 474.
- Linsky, J. L. and Avrett, E. H.: 1970, *Publ. Astron. Soc. Pacific* **82**, 169.
- Lippincott, S. L.: 1957, *Smithsonian Contrib. Astrophys.* **2**, 15.
- Liu, S. Y.: 1973, Preprint.
- Liu, S. Y., Sheeley, N. R., Jr., and Smith, E. v. P.: 1972, *Solar Phys.* **23**, 289.
- Liu, S. Y. and Smith, E. v. P.: 1972, *Solar Phys.* **24**, 301.
- Livshitz, M. A.: 1966, *Astron. Zh.* **43**, 718.
- Loughhead, R. E.: 1973, *Solar Phys.* **29**, 327.
- Lynch, D. K., Beckers, J. M., and Dunn, R. B.: 1973, *Solar Phys.* **30**, 63.
- Mein, P.: 1971, *Solar Phys.* **20**, 3.
- Michard, R.: 1956, *Ann. Astrophys.* **19**, 1.
- Michard, R.: 1959, *Ann. Astrophys.* **22**, 547.
- Mouradian, Z.: 1965, *Ann. Astrophys.* **28**, 805.
- Mouradian, Z.: 1967, *Solar Phys.* **2**, 258.
- Nikolskaya, K. I.: 1967, *Astron. Zh.* **44**, 1043.
- Nikolsky, G. M.: 1970, *Solar Phys.* **12**, 379.
- Nikolsky, G. M. and Platova, A. G.: 1971, *Solar Phys.* **18**, 403.
- Nikolsky, G. M. and Sazanov, A. A.: 1966, *Astron. Zh.* **43**, 928.
- Noyes, R. W.: 1965, in R. N. Thomas (ed.) 'Aerodynamic Phenomena in Stellar Atmospheres', *IAU Symp.* **28**, 468.
- Pasachoff, J. M.: 1970, *Solar Phys.* **12**, 202.
- Pasachoff, J. M., Noyes, R. W., and Beckers, J. M.: 1968, *Solar Phys.* **5**, 131.
- Rodionov, V. V.: 1968, *Vestn. Mosk. Univ.* **4**, 33.
- Rush, J. H. and Roberts, W. D.: 1954, *Australian J. Phys.* **7**, 230.
- Skumanich, A., Smythe, C., and Frazier, E. N.: 1972, *Bull. Amer. Astron. Soc.* **4**, 391.
- Title, A. M.: 1966, Thesis, Calif. Inst. of Tech.
- Vernazza, J. G., Avrett, E. H., and Loeser, R.: 1973, *Astrophys. J.* **184**, 605.
- Weart, S. R.: 1970, *Solar Phys.* **14**, 310.
- Wilson, A. M.: 1973, Preprint.
- Wilson, P. R.: 1970, *Solar Phys.* **15**, 139.
- Wilson, P. R. and Evans, C. D.: 1971, *Solar Phys.* **18**, 29.
- Wilson, P. R., Rees, D. E., Beckers, J. M., and Brown, D. R.: 1972, *Solar Phys.* **25**, 86.
- Zirin, H.: 1966, *The Solar Atmosphere*, Blaisdell Publ. Co., Waltham.
- Zirker, J. B.: 1962, *Astrophys. J.* **136**, 250.
- Zirker, J. B.: 1967, *Solar Phys.* **1**, 204.

## DISCUSSION

### (i) *Properties of the Chromospheric Structure as Seen in the Ca<sup>+</sup> Lines (H and K)*

There was some discussion on the relative abundance of regions with different types of H and K profiles (with single K2 peaks, double peaks, no peaks at all etc.) in spectra of the disk chromosphere (*Sivaraman, Wilson, Jensen*). *Pasachoff* pointed out that the spectrum he had analyzed was selected to show singly-peaked profiles. It was meant to demonstrate the reality of such profiles rather than to provide statistics valid for the whole Sun. *Newkirk* asked what the physical interpretation of the different kind of profiles is. The only reply to this was by *Cram* who described his view of the profiles of the supergranule center structures. He interprets the emission features called grains (greatly enhanced K<sub>2v</sub> peak) to be the results of propagating waves and shocks. The regions of completely quiet chromosphere between the grains have probably no K reversals at all (which could mean that the chromosphere there is transparent). *Cram* stresses that it is necessary to use time series of line profiles in the derivation of physical conditions. The grains, and the area in which they are embedded, show a strong 3-min oscillation in intensity (*Frazier, Zirin*), which again shows the need for a time dependence study. *Stix* points out that the 3-min period is precisely the type of period which falls just above the region in the (*k, w*) diagram where propagation is forbidden. Some inconclusive discussion followed by whether these waves therefore propagate or not (*Meyer, Frazier, Sturrock*).

### (ii) *Line Profiles of Spicules*

*Giovanelli* described spectroscopic observations by Harvey, Hall and himself of the limb in the three optically thin  $\lambda 10830$  (He),  $P_{\beta}$  (H) and  $\lambda 8542$  (Ca<sup>+</sup>) lines with 23" resolution, thus including many spicules (see also Session A discussions). They find an increase in Doppler width with height, large internal motions ( $\sim 20 \text{ km s}^{-1}$ ) and very low temperatures. *Athay* discussed the nature of the broad spectral profiles for some spicules. These, he believes, are not the result of clusters of unresolved spicules with narrow profiles, since one would expect in that case a systematically larger Doppler shift for the narrow profiled features. Often one sees the broad H and K line profiles break up in irregular, bumpy profiles (*Beckers*). The same is occasionally seen in H $\alpha$  although it is not as pronounced there because of the larger thermal width. This is even the case when spicules are observed at great heights where the chances of unresolved spicules are very small. It suggests that the emission arises from inhomogeneities within the spicule. *Schmidt* sees no theoretical difficulties in producing such an inhomogeneous-multi-component-spicule.

### (iii) *Transverse Motions of Spicules*

*Schmidt* and *Meyer* raised the point of the sideways (or transverse) motion of spicules. If the spicule consists of a 10000 km long column with  $10^{11} \text{ cm}^{-3}$  electron density in a field of a few Gauss one expects a sideways oscillation of a few minutes period (*Meyer*). *Nikolski* and *Platova* indeed claim to see oscillatory sideways motions of a few minute period (*Frazier*). *Pasachoff* pointed out that Doppler shifts seen in spicules could be due to these transverse motions (although he does not exclude the possibility of them being due to up and down motion or to a unidirectional motion along a magnetic field loop). *Zirin* and *Beckers* question the reality of the reported transverse motions of spicules. The same goes for the transverse motions (or the so called flagellant motions) reported to be associated with dark H $\alpha$  mottles on the disk (*Zirin*).